International Journal of Robotics and Control Systems
Vol. 5, No. 2, 2025, pp. 1374-1421
ISSN 2775-2658
http://pubs2.ascee.org/index.php/ijrcs

Powertrain Conversion of a Small Agricultural Tractor from Diesel Engine to Permanent Magnet Synchronous Motor

Ahmad Zaki Yaacob [a,b,1,*], Muhammad Herman Jamaluddin [b,2,*], Ahmad Zaki Shukor [b,3], Muhd Ridzuan Mansor [c,4]

[a] System Consultancy Services Sdn Bhd, 36 Jalan Wangsa Delima 6, Pusat Bandar Wangsa Maju, 53300 Kuala Lumpur, Wilayah Persekutuan, Malaysia
[b] Faculty of Electrical Technology and Engineering, Universiti Teknikal Malaysia Melaka, Hang Tuah Jaya, 76100, Durian Tunggal, Melaka, Malaysia
[c] Faculty of Mechanical Technology and Engineering, Universiti Teknikal Malaysia Melaka, Hang Tuah Jaya, 76100, Durian Tunggal, Melaka, Malaysia
[1] zaki@scs.my; [2] herman@utem.edu.my; [3] zaki@utem.edu.my; [4] muhd.ridzuan@utem.edu.my
* Corresponding Authors

ARTICLE INFO

Article history
Received March 10, 2025
Revised May 11, 2025
Accepted June 01, 2025

Keywords
Battery Dimensioning;
Powertrain Conversion;
ICE-to-Electric Conversion;
Electric Tractor;
Off-Road Vehicle

ABSTRACT

This paper presents the powertrain conversion of a small diesel-powered tractor into an electric tractor or electric off-road vehicle (EORV), offering a cost-effective alternative to purchasing a new electric model, which may be financially challenging for small-scale farmers. Given that electricity is generally cheaper than diesel fuel in Malaysia, the conversion approach aims to reduce long-term operational costs while maintaining or improving performance. The primary contribution of this work is a systematic and practical method for electric tractor conversion. The process begins with analysing the existing performance and operational requirements of the diesel tractor, followed by the selection of suitable components—namely, the electric motor, battery cells, and other associated systems. These components are then integrated into the tractor, and initial testing was performed. A speed run test was conducted to evaluate the power capability of the converted tractor. Results indicate that the electric motor delivers higher power and speed compared to the original diesel engine. The onboard energy monitoring device recorded a noticeable current spike and voltage sag during acceleration, as expected. The motor power was calculated from the recorded voltage and current data. The data show that the motor output exceeds the rated power of the original engine, suggesting that the system can handle higher loads. Some challenges encountered during the conversion process include the high initial cost, limited availability of components that meet performance requirements, and technical challenges in ensuring the durability and efficiency of the modified drivetrain. In conclusion, further testing under various load conditions is necessary to fully evaluate energy consumption and system performance in real agricultural environments.

1. Introduction

Electric vehicles (EVs) have gained widespread adoption in Malaysia and other regions due to their potential to mitigate environmental pollution and reduce reliance on fossil fuels [1]. The

Malaysian government has introduced incentives and policies to promote the adoption of EVs. This can be seen through the increasing installation of charging infrastructure and tax exemptions offered for EV purchases [2]. According to official data from the Government of Malaysia, through its website *data.gov.my*, the total number of registered EVs was 65,694 units as of March 2025. Fig. 1 shows the trend of EV registrations since 2020, which has been on an upward trajectory since 2021. Table 1 shows the yearly registrations of EVs since 2020. Based on the rate of EV registration in the first quarter of 2025, the total number of EVs registered in 2025 may surpass the number registered in 2024.

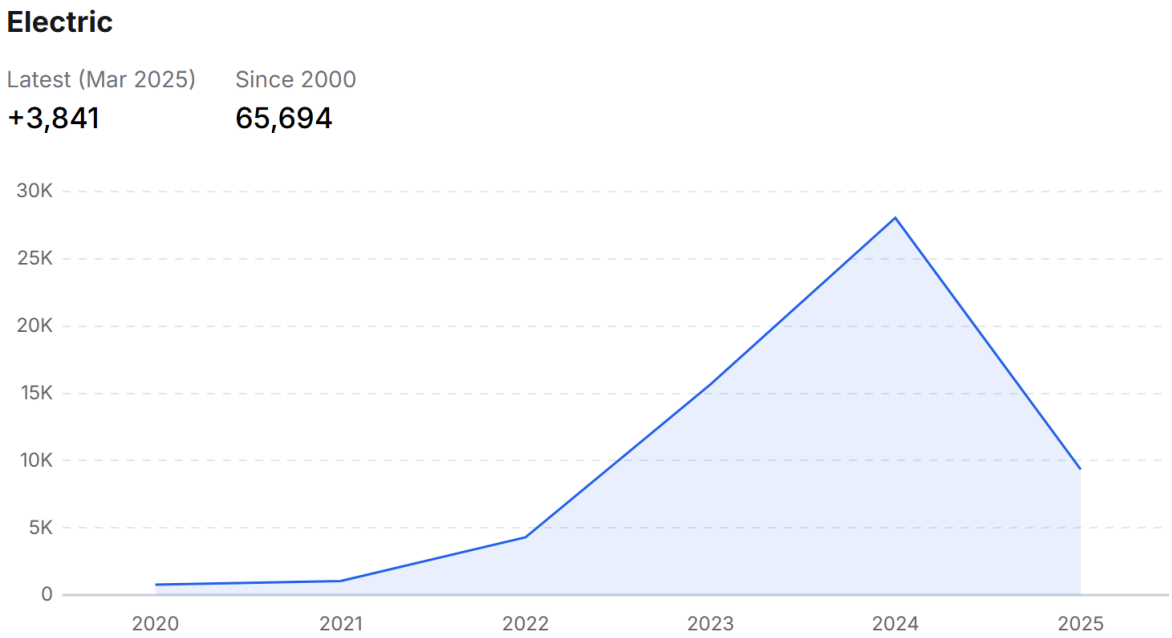

Fig. 1. EV registration yearly trend in Malaysia

Table 1. Yearly registration of EVs since 2020

Year	Total EVs registered
2020	788
2021	1058
2022	4308
2023	15669
2024	28048
2025 (end of March)	9345

There are several factors that contribute to the growth of EV adoption in Malaysia. What motivates consumers to consider EV as discussed in this paper, “Consumer Motivation to Enhance Purchase Intention Towards Electric Vehicles in Malaysia” are fuel efficiency, techno philia, perceived enjoyment, environmental concerns, and perceived environmental knowledge [3]. However, EV uptake in Malaysia remains relatively low compared to countries like Norway, the US, and China. Nevertheless, EV adoption is still gaining momentum in Malaysia due to the increase in GDP and income, which is expected to contribute to the rising number of vehicles, including electric vehicles (EVs) [4].

While much of the discussion on electrification focuses on passenger vehicles, the role of electric-powered machinery in agriculture is often overlooked [4]. There is a segment where some diesel-powered agricultural equipment, such as tractors, can be electrified to reduce emissions and fuel costs. These two problems are also the contributing factors for the adoption of electric vehicles, the environment and the rising price of energy.

There are already new electric tractors in production, such as the New Holland T4 Electric as in Fig. 2. The T4 Electric is a large tractor that falls within the mid-to-large size category. It is suitable for commercial farming operations. It is not excessively huge, but it is designed to provide the power and versatility needed for heavy-duty tasks in agriculture, making it a practical choice for farmers managing large fields. Its compact electric design, compared to traditional diesel tractors of similar power, allows it to be more efficient in terms of weight-to-power ratio and maintenance.

Fig. 2. The new holland T4 electric [5]

There is also an electric tractor sold in Malaysia called TerraGlide EV40 as in Fig. 3. Not much information is available as of today. By look, the size is smaller than the T4 Electric. While these electric tractors are readily available in the market, not all farmers are able to afford the high upfront cost of a new electric tractor. Furthermore, academic and industry research has predominantly focused on existing diesel or new electric tractor development rather than retrofitting existing diesel tractors, leaving a significant gap in systematic and cost-effective electrification strategies for conventional tractors.

From this, Universiti Teknikal Malaysia Melaka (UTeM) has initiated a retrofit project involving the conversion of an existing small-sized diesel-powered tractor into an electric-powered model. This project is called the Electric Off-Road Vehicle (EORV). The project is a collaborative effort across multiple departments, including the Faculty of Electrical Technology and Engineering, Faculty of Mechanical Technology and Engineering, Faculty of Industrial and Manufacturing Technology and Engineering, and the Faculty of Technology Management and Technopreneurship.

This paper primarily discusses the general conversion process with a focus on the electrical and electronic aspects. It covers the overall workflow, beginning with the analysis of the tractor's engine performance, the requirements and selection of EV components, and the design and fabrication of new or modified parts. It also includes the integration of mechanical, electrical, and electronic components. Upon completion, the EORV will undergo preliminary testing in a controlled private area. These initial tests will be simple in nature, as there will be further continuous improvements after the conversion.

2. Literature Review

2.1. Previous Developments

There is limited information on electric tractor conversion available. However, there are a few previous works by researchers that are similar to this research. One study was conducted by R. Melo

et al. It presents a novel 9 kW electric propulsion system for a small-scale tractor [6]. The system features two three-phase induction motors and each is driven by individual inverters. It is powered by a lead-acid battery bank and controlled via a central electronics control unit (ECU). The novel approach was the ECU, where it controls the two motors individually. The advantage from this method is the control of torque and traction. Performance evaluation through experimental drawbar tests was conducted in accordance with an international standard by Organization for Economic Co-operation and Development (OECD) CODE 2. The tests done was to investigate the performance of the drawbar pull. The experiment done demonstrates better traction and efficiency compared to internal combustion engine (ICE) tractors, highlighting the potential of electric tractors to improve productivity and reduce emissions, especially when paired with renewable energy sources.

Fig. 3. The TerraGlide EV40 Electric tractor during an agriculture exhibition in Malaysia

Another notable study is by Gautam and Dubey [7]. The research explores the conversion of a hydrocarbon-fuelled mini hand tractor into an electric-based system using a 1000 W brushless direct current (BLDC) motor. The design incorporates a high gear ratio (25:1) to achieve sufficient torque (77 Nm) for agricultural tasks, powered by a 48 V, 52 Ah lithium-ion battery. The study provides detailed calculations on power and energy requirements, highlighting the feasibility of using small electric powertrains in low-power, small-scale farming operations. It demonstrates that with proper motor selection and gearing, electric hand tractors can serve as efficient, low-emission alternatives to traditional fuel-powered models.

Another development in electric tractor technology was done by Y. Ueka *et al*. A prototype electric tractor was developed by retrofitting a 10 kW-class ICE tractor with a 10 kW alternating current (AC) motor [8]. The study emphasizes critical aspects including the tractor's specifications, energy consumption, tilling efficiency, and overall effectiveness in agricultural operations. The electric tractor showed an increase in weight; however, this had minimal impact on the vehicle's balance and stability. A key finding of the study is the significant reduction in energy consumption during both travel and tilling activities, estimated at approximately 70% compared to the original diesel-powered configuration. The electric tractor could operate continuously for approximately one hour, successfully tilling an area exceeding 1300 m² on a single battery charge. This performance

corresponds to a substantial decrease in CO_2 emissions, also estimated at around 70% relative to its ICE counterpart.

These three studies provide valuable insights into the conversion process and hardware configurations involved in electric tractor development. As noted, the hardware setups vary across the studies, including differences in motor type and rating, battery chemistry, capacity, and overall system architecture. Nonetheless, they collectively offer useful guidance for the EORV project in determining appropriate motor and battery specifications. For this EORV project, a single permanent magnet synchronous motor (PMSM) was selected, and the type of battery cells is Lithium Iron Phosphate ($LiFePO_4$).

2.2. Performance Evaluation

In terms of performance testing, K. Plizga presents a study analysing the energy performance of a tractor powered by a direct current (DC) motor [9]. The tests were different from those conducted by Y. Ueka *et al* [8]. The tests were carried out over a 100 meters distance with ten repetitions, under varying conditions, including ambient temperatures (20°C, 10°C, 0°C) and surface types (dry concrete and grass). Results show variations in voltage, current, power, energy, and driving time under different load and surface conditions. For this paper, some preliminary test shall be conducted. A full comprehensive test for the EORV shall be determined after the completion of the conversion and the initial testing.

As discussed previously, various testing methodologies were conducted. R. Melo [6] emphasizes drawbar pull performance, Y. Ueka *et al*. [8] focus on energy consumption during field operations, while K. Plizga [9] tested a tractor over a distance under varying conditions. From these studies, it can be observed that there are two main focuses of performance testing: power delivery and energy efficiency.

Besides conducting field tests, simulations were also performed for analysis. Gade and Wahab [10] present a conceptual framework for modelling and analysing the performance of an electric tractor (ET) using a PMSM. The authors develop a mathematical model of the ET based on velocity profiles typical in agricultural operations such as ploughing. A novel load-tracking control strategy is introduced, allowing for separate control of the propulsion motor's speed and torque, validated using MATLAB/SIMULINK and tested in a real-time environment via a hardware-in-the-loop (HIL) simulator. The research highlights the advantages of electric tractors over conventional ICE tractors, including reduced environmental impact and maintenance requirements. For the EORV, the tests shall be conducted in the field.

2.3. Comparative Analysis

A comparative analysis between electric and diesel tractors is also important. R. Dhond *et al*. [11] conducted a comparative analysis of electric and diesel tractors, emphasizing environmental impact, cost, and technological progress. The study underscores the urgency of transitioning to electric vehicles due to rising pollution and climate concerns. It reviews motor and battery technologies available in India for diesel-to-electric conversions and includes a cost comparison of both tractor types. The findings show the electric tractors' potential to reduce emissions and lower long-term operational costs, thus promoting sustainable agricultural practices.

Regarding the acceptance of electric tractors, Douglas *et al*. conducted a study on the potential of battery electric tractors (BETs) for small-scale organic farmers in the U.S. Midwest [12]. This research emphasizes on benefits such as improved efficiency, lower maintenance and reduced emissions compared to diesel tractors. Through interviews with 14 organic growers, the study explores perceptions and adoption barriers. While many farmers express environmental motivation and a willingness to pay more for BETs, concerns remain regarding battery capacity, maintenance costs, and long-term reliability. The study concludes that wider adoption may depend on financial incentives to offset the high initial investment.

2.4. Conversion Cost and Challenges

On the cost of a conversion, a cost model has been developed by H. Gao and J. Xue [13]. A cost model for converting diesel-powered agricultural tractors to electric tractors was proposed, emphasizing economic evaluation through life cycle cost analysis, sensitivity analysis, and the incremental payback period (IPBP). The total conversion cost increases notably with higher power demands, primarily due to limitations in battery weight, volume, and operational duration. Although the initial investment for electric tractor conversion may be two to five times greater than the diesel tractors, the life cycle cost is estimated at approximately 60% of that of diesel, particularly under stable agricultural electricity tariffs and declining battery costs driven by technological progress. The analysis suggests that lower-power conversions offer the most cost-effective solutions, while higher-power applications pose affordability challenges for typical farmers.

There are several challenges in ensuring the success of the conversion. The hardware setup and conversion process differ for each tractor model, as every model has its own dimensions, weight, and powertrain configuration. Electrical components, such as electric motors, must match the diesel engine in terms of power and torque. The challenge lies in identifying the optimal motor performance at an acceptable cost. The battery pack must also be dimensioned according to the motor's performance and the desired range, to ensure proper matching between the motor and the battery pack.

The choice of $LiFePO_4$ battery cells in this research is necessary. Although the battery has lower energy density compared to ternary lithium-ion batteries which may limit driving range [14], it offers enhanced safety characteristics [15]. Battery safety is attributed to the thermal and chemical stability of lithium iron phosphate materials, which significantly reduces the risk of fire or explosion, even under high-temperature conditions or during short circuits [16]. Furthermore, the cost of LFP batteries is considerably lower than that of ternary batteries [14]. In addition to the cost, it has long lifecycle [14]. For this EORV project, the two key advantages, safety and cost, are of paramount importance.

In terms of mechanical fabrication and modifications, there shall be some challenges in designing parts. Some parts shall be fabricated or modified, for example, the motor mount and the motor coupler. The parts must be carefully designed to ensure the integrity of the components. This is important for drivetrain integration with the motor. The placement of new components may also affect the stability of the tractor in terms of weight and weight distribution.

Besides the technical challenges, the initial cost of retrofitting an electric motor to an existing diesel-powered tractor can be significant. Depending on the system configuration, the battery pack and motor represent the most significant cost components influencing the overall expenditure. As previously discussed, a low-power setup is generally more favourable; however, for high-power setup this can be offset by long-term returns on investment.

Having discussed all key aspects of the conversion process, the research contribution of this research is the systematic conversion of a small agricultural tractor from an internal combustion engine to a permanent magnet synchronous motor (PMSM) powertrain. The conversion shall be carried out through a practical and cost-effective approach, aimed at demonstrating its feasibility for real-world applications. Furthermore, this research offers a potential solution to the increasing environmental concerns associated with conventional agricultural machinery [17].

3. Benefits of Conversion

The primary goal of this project is to convert an existing diesel-powered tractor into an electric-powered model. This approach offers several benefits, as discussed in the following sections.

- It provides a more cost-effective solution compared to purchasing a brand-new electric tractor, making it more accessible for smaller-scale farmers.
- It reduces the environmental impact by replacing the diesel engine with an electric motor, lowering emissions and noise levels.

- It has better energy efficiency that can provide further cost savings.

By converting diesel tractors to electric, farmers can gain benefits like better energy efficiency, lower operating and maintenance costs, and smaller environmental footprint, without the high upfront investment required for a new electric model [18].

3.1. Cost Reduction

Several studies have compared the cost of ownership between battery electric vehicles (BEVs) and internal combustion engine (ICE) vehicles [19]. But this is only applicable to passenger vehicles. Electric tractor is something else because compared to passenger cars, there are only a fraction of them compared to passenger cars. Furthermore, the functions are different than passenger cars. The cost of purchasing a brand-new electric tractor can be a significant barrier for many farmers, particularly those with smaller operations or limited financial resources. As discussed in literature review, the overall cost for electric tractors significantly lower in the long run.

Cost savings depend on several factors. Firstly, the powertrains for the tractors must be compatible in terms of physical and performance. The retrofitted parts must be mechanically integrated with minimum modifications. The powertrain consists of an electric motor, a motor controller and a battery pack. These three components are the major part in any electric vehicle. Caution must be made so that the initial cost and the powertrain configuration contribute the most to the overall cost [20]. The powertrain configuration must be designed to ensure that the cost savings in the long run are maximized without compromising performance or reliability. Additionally, the conversion process can be carried out by the farmer or a local workshop, further reducing the overall cost compared to acquiring a factory-produced electric tractor.

Secondly, operating costs are lower because electricity is generally cheaper than fuel in Malaysia [21]. The literature review also indicates that operating an electric tractor is generally more cost-effective compared to its ICE counterpart. To provide a comparative perspective, the operating costs of a battery electric vehicle (BEV) will be evaluated against those of an ICE vehicle. For example, a Hyundai Kona electric that has 39.2kWh battery pack and can go up to 305km (WLTP) on a single charge. If the car is charged at home, using the maximum electricity tariff rate in Malaysia for domestic consumers of RM0.57 per kWh, the cost to charge the 39.2kWh battery pack will be RM22.38. However, charging losses and inefficiencies of the onboard charger (OBC) was not included. Based on several studies, the OBC efficiency can be above 95% [22]-[24]. Assuming the efficiency is 90%, the actual energy that is required to charge the battery pack will be $39.2kWh/0.9 = 43.56kWh$, and that will cost RM24.83. Therefore, in terms of cost per 100km, the cost for 100km range will be **RM8.17/100km**.

In comparison to a popular Malaysian national car Perodua Myvi, that uses subsidized petrol, the published fuel consumption is 21.1km/L or 4.74L/100km. Perodua Myvi is a class B vehicle that is slightly smaller than Hyundai Kona. However, this published number is a bit optimistic which will be discussed in the next paragraph. At the current moment, the RON95 petrol price is RM2.05/L. In terms of cost per 100km, it will be **RM9.72/100km**. In comparison, the energy cost for Hyundai Kona per 100km is cheaper. Without fuel subsidy, especially diesel, the fuel cost per Liter for Perodua Myvi will be more than RM3 per Liter and the cost per 100km will be more than RM10/100km.

Here is some discussion on the published number by the manufacturer for energy consumption and fuel consumption. For BEVs, WLTP or Worldwide Harmonized Light Vehicles Test Procedure, is a test cycle procedure for manufacturers to publish the energy consumption of a vehicle. WLTP has stricter parameters that the published parameters of BEVs are generally considered to be more realistic compared to other standards [25]. One study in Europe compares the real-world fuel consumption against publish numbers of ICE vehicles and BEVs. The average energy consumption values for ICE are significant that the real-world tests can be 18% higher than the published values. BEVs on the other hand have an average of 2.6% and in some instances a range of 0.3% to 4.6% above manufacturer published value [26]. One study in China highlights that, the discrepancies of between published fuel consumption against real world fuel consumption can be up to 25% [27].

Therefore, by comparing and referring to manufacturer published numbers and the research papers, the cost to operate a BEV is cheaper than ICE [28]. From a long-term perspective, the electricity savings potentially can improve the operating cost for the farmers.

Thirdly, the maintenance would be cheaper and easier. Besides tyre maintenance, there is no maintenance for engine oil, filters and timing belts. It has fewer moving parts in an electric motor compared to a diesel engine [29]. A study shows that the cost of owning and operating tractors is a significant component of agricultural production costs, representing approximately 35% to 50% of the total agricultural production costs, excluding land expenses. This encompasses various costs, including depreciation, insurance, maintenance, repairs, fuel, and labour costs associated with tractor operation [30].

Having discussed these three points, it can be concluded that the overall cost shall be cheaper for farmers. With a careful planning, the conversion of a diesel tractor to an electric tractor can be a cost-effective approach. The cost of conversion may be high initially, but it is also dependent on the configuration of the power train. In the long run, overall operating cost and maintenance cost will be cheaper.

3.2. Environmental Impact

The environmental impact of agricultural machinery is a growing concern, as diesel-powered tractors significantly contribute to greenhouse gas emissions and air pollution [31]-[36]. The conversion of a diesel tractor to an electric model can substantially reduce the environmental footprint of agricultural operations. With zero emissions, electric tractors do not generate any tailpipe emissions [37], effectively eliminating the release of harmful pollutants such as nitrogen oxides, particulate matter, and carbon monoxide into the atmosphere.

Diesel exhaust has several pollutants that are dangerous to health. These pollutants can be categorized into gaseous emissions, particulate matter, and other toxic compounds. The publication Diesel and Gasoline Engine Exhausts and Some Nitroarenes by the International Agency for Research on Cancer (IARC) provides a comprehensive evaluation of the composition, emissions, and potential health risks associated with diesel and gasoline engine exhausts [38]. It discusses in detail engine types and combustion processes, emissions composition, health implications, and regulatory and technological developments. Furthermore, it underscores the importance of continued efforts to minimize emissions from ICE vehicles to protect public health and the environment. The EORV project can contribute to this effort by converting an existing diesel tractor to a cleaner, more environmentally friendly electric model that eliminates these harmful emissions.

Besides these harmful gas and particle emissions, the reduction in noise levels is another significant environmental benefit of electric tractors. Diesel engines typically generate high levels of noise pollution, which can be disruptive to both workers and nearby communities [39]. Electric motors, on the other hand, are quieter comparatively, providing a more comfortable work environment and reducing the impact on surrounding areas.

One pressing issue concerning EVs is the end-of-life management of the batteries. In this regard, several studies have focused for battery recycling. A study by A. Zanoletti *et al*. [40] discussed the need of effective recycling to manage waste and address critical raw material supply issues. It also evaluates recycling technologies such as pyrometallurgy, hydrometallurgy, biometallurgy, and solvometallurgy. These technologies are discussed in terms of efficiency, environmental impact, and technical maturity. Among them, hydrometallurgy emerges as the most favourable option due to its low energy consumption, high product purity, and high recovery rate. However, it produces a significant amount of wastewater as a drawback.

One study discusses and reviews the lithium-ion battery recycling process from a circular economy perspective [41]. A circular economy is an economic system that focuses on eliminating waste and keeping resources in use for as long as possible. It promotes the reuse, refurbishment, and recycling of resources. The paper identifies two primary alternatives to battery disposal: recycling and

second-life applications. These two approaches offer solutions to reduce toxic waste and minimize environmental impact.

Another similar study by L. Toro *et al*. [42] discusses existing battery recycling methods, including mechanical, pyrometallurgical, and hydrometallurgical processes, highlighting their strengths and limitations. It also examines the challenges faced by the industry, such as high costs, environmental impacts, and safety concerns. Future prospects for advancements in battery recycling technologies are explored, with a focus on integration into a circular economy, enhanced collection and sorting techniques, and the potential development of innovative recycling processes.

There are advantages and disadvantages in making the secondary use of batteries. Based on a review by H. Yang *et al*. [43] which discusses the secondary use and recycling of lithium-ion batteries from electric cars, giving a second life to batteries can benefit the environment by reducing pollutants and increasing energy efficiency. On the other hand, there are some drawbacks. The required infrastructure can be complex and costly, and there are additional costs associated with the processing and testing of used batteries.

While the discussion on battery recycling is on lithium-ion batteries, there is a study on recycling and treatment of spent $LiFePO_4$ batteries in China. W. Wang and Y. Wu [44] highlight the challenges in recycling these batteries, as they do not contain precious metals, making the traditional recycling processes complex and inefficient. It also discusses the recovery and recycling methods that include vacuum treatment, hydrometallurgical processes, regeneration of active materials and carbothermal reduction and electrochemical methods.

Based on the discussions, the transition from diesel to electric tractors offers a viable solution for reducing environmental impact in agricultural settings. The zero tailpipe emissions and the reduced noise levels of electric motors contribute to a more sustainable and environmentally friendly agricultural practice. Furthermore, strategies for managing end-of-life batteries have already been proposed, including repurposing and recycling methods that align with the principles of a circular economy. While these solutions offer promising pathways for sustainability, their widespread adoption and implementation on a global scale will require time, supportive infrastructure, and regulatory alignment.

3.3. More Efficient Energy Utilization

The conversion of a diesel-powered tractor to an electric model can lead to a significant improvement in energy efficiency. In general, electric motors are more efficient than any ICE vehicles. Theoretically, electric motors have greater than 85% efficiency of transforming electricity to mechanical energy. One study observed that brushless DC motors (BLDC) give the best energy efficiency (greater than 95%) followed by induction motors (greater than 90%) [45].

On the other hand, modern diesel engines can achieve thermal efficiencies of 35% [46]. The rest of the energy becomes wasted as heat. One advantage of electric motors is that it will only consume energy when performing useful work, unlike a diesel engine which will continue to consume fuel even if the tractor is idle. It doesn't have engine auto START-STOP feature like some modern cars have.

While converting a tractor powertrain from an internal combustion engine (ICE) to electric improves energy efficiency, there are also disadvantages. Batteries have lower energy density compared to fuel. Although the converted vehicle may maintain similar performance as before, it may experience reduced driving dynamics due to the increased weight of the battery pack. Or it may also retain similar dynamic characteristics and weight balance; however, the overall range is reduced because of the limited energy capacity of the battery. Therefore, it is critical to understand the overall requirements, including the tractor's operational demands and intended purpose.

In summary, the conversion of existing diesel-powered tractors to electric models offers several key advantages, including reduced operating costs, lower environmental impact and improved energy efficiency. These advantages are further realized when renewable energy sources like solar power are used for charging, thereby supporting a comprehensive sustainable strategy. These advantages make

electric tractors a promising solution for more sustainable agricultural practices. However, such advantages can only be fully realized if all operational, technical and economic requirements are carefully considered and well balanced during the planning and implementation stages.

4. Development Method

The development of the tractor can be divided into several categories and stages. The straightforward approach is to divide the work based on the EV components, mechanical work, and electrical and electronic integration. Some of these can be done concurrently while others may have to wait for others to complete. Fig. 4 shows a diagram of the development of the electric tractor.

The process commenced with requirement analysis, encompassing the initial design phase and the evaluation of feasibility and structural modifications. Extensive research was undertaken to identify and to select appropriate electric vehicle (EV) components, including the PMSM, battery pack, motor controller, and onboard charger (OBC). While procurement was in progress, mechanical components requiring fabrication and modification to accommodate the new powertrain and battery system were prepared based on manufacturers information and schematic diagrams. When all components were complete, system integration was performed. Preliminary testing was then conducted to evaluate drivability, with a focus on torque delivery, handling, and overall system performance, ensuring the converted tractor met functional and operational criteria.

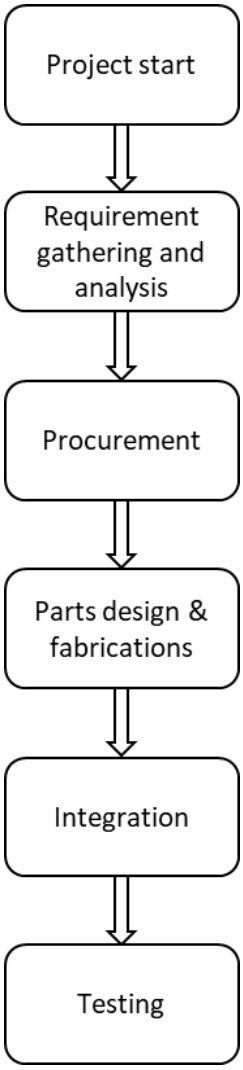

Fig. 4. Project flow diagram

Given the multidisciplinary nature of this project, the research involved collaboration across multiple faculties and departments. This paper focuses on key aspects of the conversion process, including powertrain requirements, electrical and electronics integration, and preliminary performance testing. In the following sections, requirement gathering and analysis were conducted on the tractor platform, existing diesel engine, electric motor requirements, battery cell requirements, and other electronic components. After all these requirements are identified, a design process will be carried out for the mechanical parts and components. Upon the arrival of all components, the mechanical parts and electrical and electronic components will be integrated.

4.1. Tractor Platform

The tractor platform is based on an existing tractor, the Kubota B7000D. This is a compact utility tractor with a 4-cylinder water-cooled diesel engine. It is a compact, versatile 4WD tractor that could cater to small-scale farms, orchards, and gardens. It has 6 forward gears and 2 reverse gears. Users can select 2WD or 4WD modes. The weight of the tractor is 475 kg.

It is an old model tractor which was produced in the 1970's. The tractor is no longer in production. However, there are workshops that can maintain the tractor and the spare parts are still available today in the market. Fig. 5 is a picture of the tractor and Table 2 is the specifications of the tractor.

Fig. 5. The Kubota B7000D

Table 2. The Kubota B7000D engine specifications

Items	Parameters
Model	Kubota Z650
Type	4-cycle two-cylinder water-cooled diesel
Number of cylinders	2
Displacement	0.61 liters
Bore	76.0 mm
Stroke	82.0 mm
Aspiration	Naturally aspirated
Rated Engine Power	14.0 hp (10.4 kW) at 3000rpm
Maximum Torque	29.2 Nm (21.6 lbs-ft) at 1800rpm
Compression Ratio	21:1
Fuel Tank Capacity	15.0 liters

Based on the specifications, the engine displacement is 0.61 ℓ, and it can produce 10.4 kW power at 3000 RPM (revolutions per minute). From this information, the torque at this RPM is 33.1 Nm by using the following formula:

$$P = \tau \times 2\pi \times (RPM/60) \quad (1)$$

Where

P : is the power in watts

T : is the torque in newton-meters

RPM : is the engine revolutions per minute

Rearranging the formula to:

$\tau = (P \times 60)/(2\pi \times RPM)$

$\tau = (10.4 \times 60)/(2\pi \times 3000)$

$\tau = 33.1\ Nm$

From the specifications sheet, when the engine is at 1800 RPM, it produces 29.2 Nm of torque. Using the equation (1), the power at 1800 RPM is calculated to be 5.5 kW.

$P = 29.2 \times 2\pi \times (1800/60)$

$P = 5.5$ kW

From here, a power-torque against engine speed graph can be generated. It is not a complete picture of the power-torque chart, but it is useful to visualize the electric motor performance, and it is useful in selecting the right electric motor. Fig. 6 shows the power-torque graph for the Kubota B7000D diesel engine.

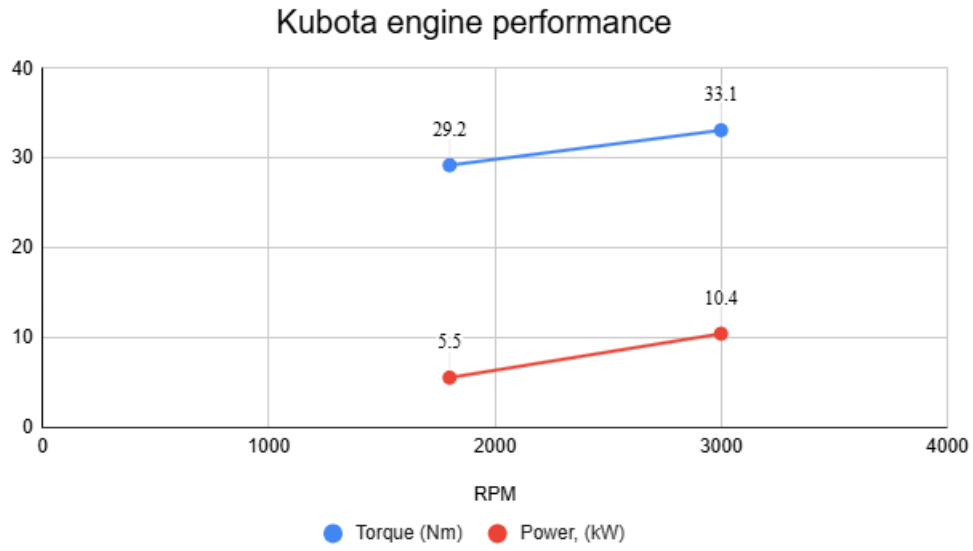

Fig. 6. The Kubota B7000D engine performance graph

From the graph in Fig. 6, the torque and power lines are still climbing. From the specifications, the power specified is rated, not maximum power. For a typical ICE, the peak torque occurs before maximum power. Fig. 7 shows an example of a diesel engine dyno chart. The curve on top of the graph is torque and the curve in the graph is power. Notice that the torque reaches its peak while the power is still climbing.

ICE torque curve typically has inverted `U' shape [47], [48]. Modern engines with variable valve technology have flatter torque curve [49]. In actual Kubota B700D engine performance curve, it shall have similar shape in Fig. 7. The information supplied by the manufacturer may not be sufficient, but it is essential that the power rating and torque of the electric motor are available.

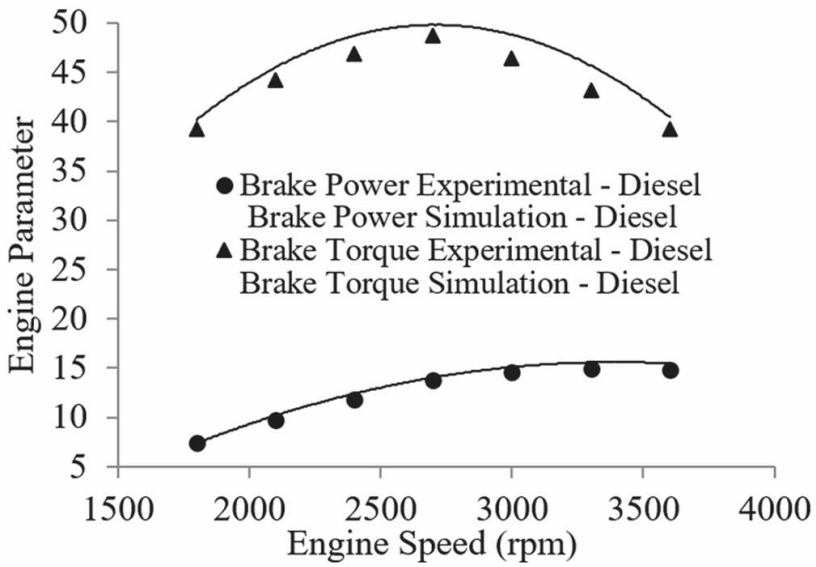

Fig. 7. Engine performance chart [Image from: "Analysis of Internal Combustion Engine Performance Using Design of Experiment,". Licensed under CC BY 4.0] [47]

4.2. Powertrain Design and Requirement

The fundamental objective of the powertrain design is to ensure that the electric tractor can deliver the same or better performance compared to the original diesel version. There is a study that emphasizes power design, especially on electric motor performance. The aim of the design is to achieve similar or improved performance compared to traditional diesel-powered tractors [50]. To achieve this, the electric motor selection and battery sizing need to match the capability of the diesel engine.

4.2.1. Electric Motor

Based on the information gathered from the diesel engine specification, the electric powertrain design will consider the following:

- Electric motor that is capable to spin to at least 3000 RPM.
- Electric motor with power output of 10 kW.
- Electric motor with torque output of 30 Nm.
- Electric motor can be either Brushless DC motor (BLDC) or Permanent Magnet Synchronous motor (PMSM).

The two popular electric motors that are available on the market are BLDC and PMSM motors. There are several studies on these two types of electric motors. However, the study shows that PMSM is generally efficient and can achieve more range for a light electric vehicle as compared to BLDC motors [51].

The torque curve of an electric motor is flat across a wide RPM range unlike ICE. As mentioned by a study, electric motors have maximum torque across a wide speed range while diesel engines have high torque at a smaller window RPM. At low speeds, the torque from a diesel engine is about 30% of its nominal value [52], while electric motors can have the maximum torque at low speed. The following Fig. 8 is an example of a typical torque-speed graph of an electric motor [53]. The initial torque is at the highest point as compared to diesel engines.

One key advantage of electric motors is their ability to deliver high torque at low RPM [54], [55], which is ideal for tractor applications. One electric motor was identified for this conversion. It is an 8000 W PMSM motor. This electric motor is meant for off-road dirt bikes. Fig. 9 shows a picture of the PMSM motor. It can be powered by a 60 V up to 96 V power supply. The weight of the electric

motor is 21 kg. The electric motor power is rated at 8 kW and is able to deliver maximum output of 15 kW. The rated torque is 18.2 Nm and the peak torque can reach up to 65 Nm. This is twice the torque of the tractor's diesel engine. The rated speed of this electric motor is 4200 RPM and can peak at 6000 RPM. This electric motor specification matches well with the diesel engine capabilities of the Kubota B7000D tractor. The following Table 3 is the specifications of the PMSM motor.

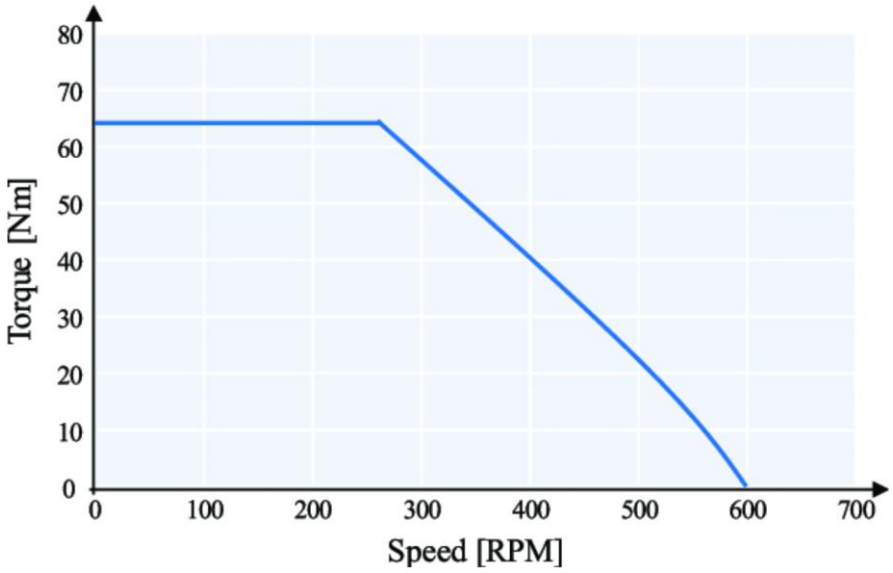

Fig. 8. Drive motor torque speed curve (Adapted from K. Lee and M. Lee) [Licensed under CC BY 4.0] [53]

Fig. 9. A picture of the PMSM motor

Table 3. Specifications of the PMSM motor

Item	Parameters
Nominal battery voltage, V	72
Rated power, kW	8
Peak power, kW	15
Rated speed, rpm	4200
Peak speed, rpm	6000
Rated torque, Nm	18.2
Peak torque, Nm	65 (0~4000 rpm)
Rated battery current, A	73
Maximum line current, A	160
Maximum phase current, A	450

From the electric motor specifications, a comparison between the Kubota engine and PMSM motor has been made. Table 4 shows the comparison of the performance in terms of power, torque and speed.

Table 4. Performance comparison between Kubota engine and PMSM motor

	Kubota Engine	PMSM motor
Rated power (kW)	10.4	8
Max power (kW)	Not Available	15
Max torque (Nm)	33.1	65
Rated RPM	3000	4200
Maximum RPM	Not Available	6000

To visualize the performance differences, the following Fig. 10 is the power-torque curve comparison between the diesel engine and the selected electric motor. This is not the exact real performance curve, but it illustrates the performance of using an electric motor for the tractor based on the parameters available. There are some assumptions that have been made. The torque curve is flat from zero to 4200 RPM. The torque value is derived from the maximum power of the PMSM motor which is 15 kW. Therefore, using equation (1), the torque is 34.1 Nm.

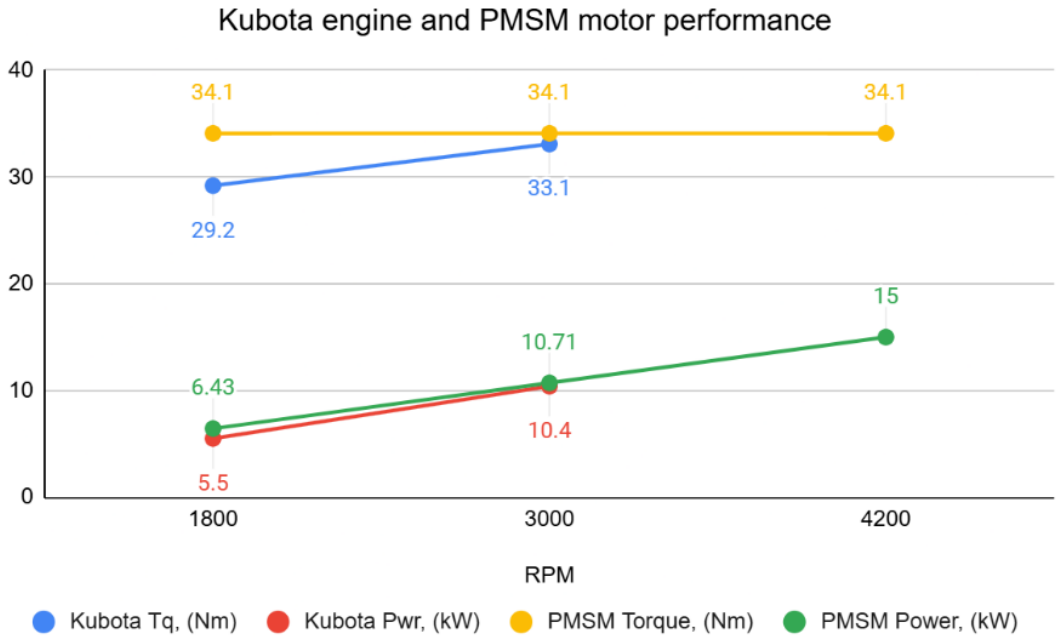

Fig. 10. Performance comparison chart between Kubota engine and PMSM motor

4.2.2. Motor Controller

The PMSM comes with a matching motor controller or inverter. The motor controller is responsible for the operation of the electric motor by controlling the voltage, current and frequency supplied to the electric motor [56]. The motor controller is rated at 72 V nominal that can handle up to 850 A peak current and 350 A continuous current. In terms of electrical power, the motor controller can deliver 61.2 kW of peak power and 25.2 kW of continuous power. That is more than enough to meet the required performance of the electric motor. The following Fig. 11 is a picture of the motor controller. Table 5 shows the specification of the motor controller.

There are programmable settings that can be adjusted in the controller to optimize the performance according to the tractor's requirements. Adjustable settings include battery limits, current

limits, temperature limits, electric motor rotation, throttle response, speed limit, regenerative braking and torque control. There is also a more advanced speed control for this electric motor for advanced users that requires PI (Proportional-Integral) settings [57]. With this customizability, the performance and the protection of the electric motor can be set to suit the tractor application.

Fig. 11. The motor controller

Table 5. The motor controller specifications

	Specifications
Operating voltage (V)	48/50/72
Maximum voltage (V)	88
Phase current (A)	850
Line current (A)	450
Motor power (kW)	6-8
IP rating	IP67
Net weight (kg)	3.08

4.2.3. Battery Pack

The battery pack size is determined by the energy required for the tractor operation. For this conversion, the $LiFePO_4$ battery cells were selected. The $LiFePO_4$ has less energy density than other Lithium-Ion variants, but it provides better safety [58]. There are two criteria to consider when sizing the battery pack:

- The electric motor operating voltage and current requirement.
- The duration or range of the tractor operation on a single charge.

4.2.4. Motor Voltage and Current Requirement

The selected motor controller can accept voltage of up to 88 V (refer Table 5). To meet the voltage requirement, some calculations are needed. Based on manufacturer data, the minimum and maximum voltage of the $LiFePO_4$ batteries is 2.5 V and 3.65 V respectively (refer Fig. 12). Using the fully charged voltage of 3.65 V, we can determine the number of cells needed: $88\,V\ /\ 3.65\,V\ =\ 24.1$ cells in series. The number shall be round down to 24 cells. Therefore, the actual battery pack voltage will be, $24\ \times\ 3.65\,V\ =\ 87.6\,V$. From this, the lowest voltage of the battery pack can be determined, $24\ cells\ \times 2.5\,V\ =\ 60\,V$.

The minimum and maximum voltage of the battery pack shall meet the motor controller operating voltage. Refer to Table 5 in the previous subtopic.

2 Description and Model

2.1 Description: LFP Li-ion Power Battery with aluminum shell.

2.2 Model: LF230.

3 General Technical Parameter

No.	Item		Parameter	Remark
1	Typical Capacity		230Ah	(25±2)℃, Standard charge and discharge
2	Typical Voltage		3.2V	
3	AC Impedance Resistance		≤0.30mΩ	
4	Standard charge and discharge	Charge/Discharge Current	0.5C/0.5C	(25±2)℃
		Charge/Discharge Cut-off Voltage	3.65V/2.5V	
5	Max Charge/Discharge Current	Continuous Charge/Discharge Current	1C/1C	Reference Continuous/Pulse Charge/Discharge Current Map
		Pulse Charge/Discharge Ccurrent（30s）	2C/2C	
6	Recommended SOC window		10%～90%	N.A.
7	Charging Working Temperature		0℃～60℃	Reference Continuous/Pulse Charge/Discharge Current Map
8	Discharging Working Temperature		-30℃～60℃	
9	Storage Temperature	Short Term(Within a Month)	-20℃～45℃	N.A.

Fig. 12. Battery cell specifications from the manufacturer

For current requirement, the motor controller can handle up to 450 A continuous and 850 A peak. The continuous current value indirectly will be used to determine the battery capacity. This is due to the C-rate of the battery is related to the capacity of the battery. The C-rate of the battery is a measure of the rate at which a battery can be charged or discharged relative to its capacity [59]. The manufacturer specification sheet shall provide the C-rate value of the battery. Different batteries have different charging and discharging rates. Incorrect match of the charging & discharging rate of a battery will give capacity fade and severe voltage drop under load. Capacity fade refers to the reduction in the total capacity that can be stored and delivered by the battery over its lifetime [60]. The following is the C-rate formula.

$$C - rate = (Discharged\ current\ /\ Battery\ capacity) \quad (2)$$

Or

$$C - rate = (Charge\ current\ /\ Battery\ capacity) \quad (3)$$

The higher the C-rate the quicker the current can be charged or discharged, vice versa. For the EORV, $LiFePO_4$ batteries with 230 Ah have been selected as in Fig. 11. The discharging rate is critical

as this determines whether the battery can supply sufficient current to the motor controller and the electric motor. Based on the manufacturer data, the 230 Ah battery cell has a discharging C-rate of 2C and charging rate of 1C. Therefore, the battery is capable of discharging current continuously at 460 A. Compared to the motor controller specifications in Table 5, the line current that the motor controller can handle is 450 A. Thus, these battery specifications shall meet the motor controller requirement. However, for charging, the manufacturer recommends charging at 0.5C or slower (115 A or lower). From the data, the maximum power output from the battery pack which is $87.6\,V \times 460\,A = 40.3\,kW$. This is the theoretical value of the maximum power that the battery pack can provide.

4.2.5. The Duration or Range of the Tractor Operation on a Single Charge

The next step would be to estimate the energy requirement for a typical tractor operation. A typical tractor working time is usually 8 hours per day for ploughing, harrowing, seeding and other farm work [61]. At the current moment, there is no data on the fuel consumption on the diesel-powered tractor. There is no data on how long the engine with full tank fuel will last. However, the energy requirement was estimated based on the fuel tank of the tractor which is 15L. This calculation is a simple estimation where external factors are not included such as operation type, operation duration and terrain condition.

According to the U.S. Department of Energy's Alternative Fuels Data Centre, diesel has an energy content of approximately 36.0 megajoules per liter (MJ/L) [62]. Therefore, the total energy content in the diesel tractor's fuel tank is $15\,L \times 36.0\,MJ/L = 540\,MJ$. To convert from MJ/L to kWh, the following equation is used.

$$Energy\ in\ kWh = Energy\ in\ MJ \times 0.2778$$

$$Energy\ in\ kWh = 540 \times 0.2778$$

$$Energy\ in\ kWh = 150.012\,kWh$$

From the calculation, the total energy content for a 15 L tank is 150 kWh. This number however is too big for a battery pack.

It is important to note that this figure assumes 100% efficiency, which is unrealistic. This figure must include diesel engine efficiency and electric motor efficiency. Assuming the diesel engine efficiency is 30% and the electric motor efficiency is 90%, as mentioned in the earlier topic, calculated energy from the battery pack would be,

Usable energy from 15 litre diesel, $150\,kWh \times 30\% = 45\,kWh$

Required energy for the electric motor $45\,kWh\ /\ 90\% = 50\,kWh$

According to the analysis, the tractor conversion can be designed with a **50 kWh** battery pack.

Based on the 230 Ah battery pack data, the total battery energy can be calculated.

$$Battery\ energy = Battery\ nominal\ voltage \times Battery\ capacity$$

$$Battery\ energy = 87.6V \times 230\,Ah = \mathbf{20.1\,kWh}$$

The difference between 50 kWh and 20.1 kWh is huge. The battery pack is less than half the capacity of the requirement. However, the current battery was selected based on constraints such as physical space, weight, cost, and proof-of-concept testing objectives. In terms of operation, the electric tractor shall be more efficient as the electric motors don't consume much energy than the diesel engines when idle. Moreover, not all farm operations require continuous 8-hour use; some lighter-duty tasks or shorter shifts may be supported by the current capacity.

This is an opportunity for researchers to further study the energy consumption [63], [64]. As part of this research, actual energy consumption testing shall be conducted to improve the accuracy of the estimated energy requirements and to evaluate the real-world performance of the electric tractor. The calculated battery capacity is simplified and it relies on theoretical energy equivalence than real data.

The performance in real-world conditions is significantly influenced by operator behaviour and varying terrain characteristics commonly encountered in agricultural environments. Further work is planned to monitor the actual energy consumption under real agricultural working conditions, as what has been discussed in the literature review, to better understand the performance and to validate battery sizing.

4.2.6. Battery Management System and Onboard charger

The battery management system (BMS) and the onboard charger (OBC) are components for the battery pack. BMS monitors and manages the battery pack to ensure safety, prolong the battery life and improve battery efficiency [65]. The BMS is from off-the-shelve product. It is a 24s BMS from Dongguan Daly Electronics Co. Ltd. Similar to the motor controller, it has programmable settings for over/under voltage, over current, temperature, state-of-charge and more. This will be covered in a later topic.

The OBC is an AC to DC type charger, and it has an output of 6 kW power. With the 20.1 kWh battery pack, the charge time for the tractor battery will be 3.35 hours from zero capacity. The following Fig. 13 shows the block diagram of BMS and onboard charger for the battery pack. Fig. 14 and Fig. 15 show the pictures of OBC and BMS.

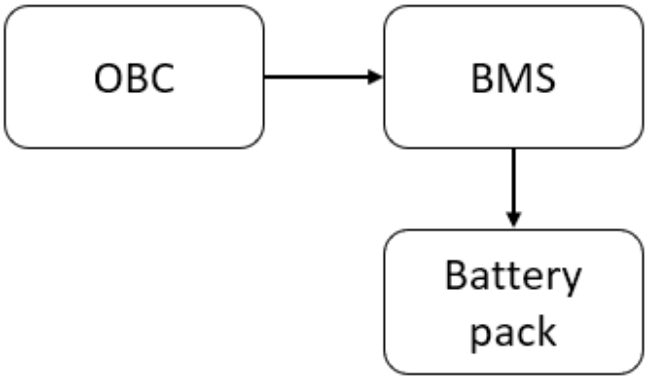

Fig. 13. Block diagram of OBC, BMS and battery pack

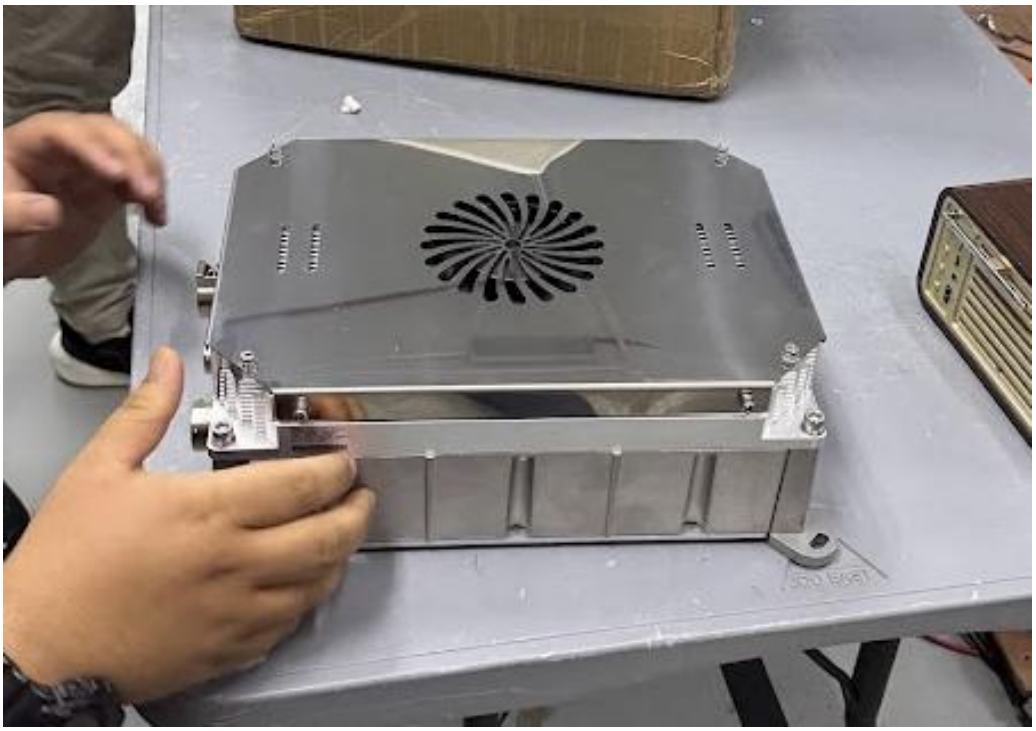

Fig. 14. The onboard charger

Fig. 15. The BMS for this project

4.3. Other Electronics Components

Other electronic components in the electric tractor conversion include the pre-charged circuit and disconnects such as the contactor. The contactor is a high-power electromechanical device used to switch electrical circuits on and off. For the electric tractor, there are three disconnects: a maintenance switch, a breaker, and a contactor.

The maintenance switch on Fig. 16 is a manual switch that is only operated by hand. This switch will break all electrical connections to the battery. The breaker is similar to any DC breakers that protect the circuit. The contactor is a switch like relays that are activated by magnetic coil as in Fig. 17. The function is to turn on the motor controller and the rest of the electrical system.

Fig. 16. The main/maintenance switch

Fig. 17. A contactor can carry bigger current than a typical relay

However, the contactor must be paired with a pre-charge circuit to limit the inrush current to the motor controller. The pre-charge circuit bypasses the contactor from the battery pack to the motor controller. It contains a resistor that limits the current to charge the capacitors inside the motor controller. Once the capacitors are charged, the contactor can then be activated. A contactor that is activated without a pre-charge circuit may be exposed to failures due to burning contact points inside and electric arcs of the inrush current from the battery to the motor controller [66]. Fig. 18 shows a basic circuit diagram for the contactor.

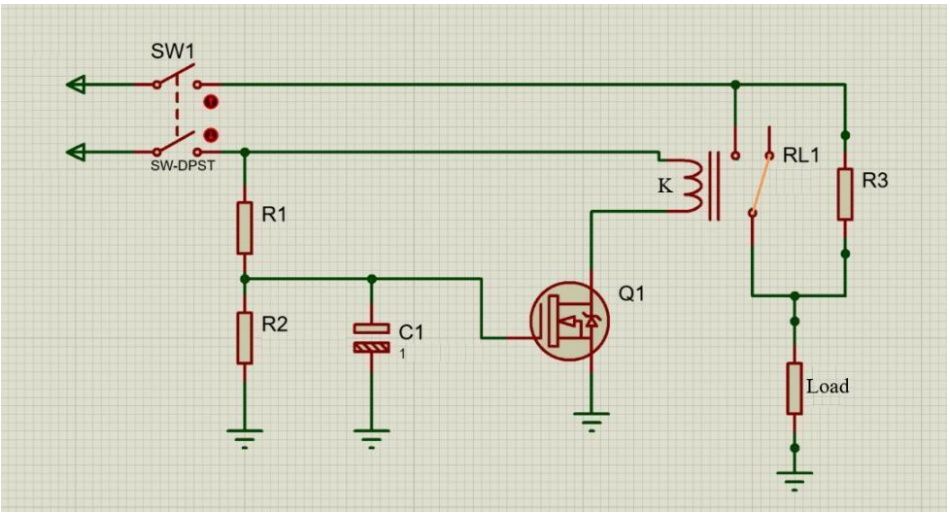

Fig. 18. The overall circuit for switch, contactor and pre-charge circuit

This is a basic diagram for a switch and a contactor with a pre-charge circuit. On the left side is a double-pole, single-throw (DPST) mechanical switch. The contactor is denoted as K and is connected to the power source through the normally open port. Resistor R3 is the pre-charge resistor, and the load on the bottom right is the motor controller. R1, R2, C1, and Q1 in the middle of the circuit represent resistors, a capacitor, and a MOSFET, respectively. These components function as a delay circuit to drive the coil in the contactor (K).

When the switch (SW1) is closed, current will flow through R3 and the delay circuit. The current flowing to the motor controller is initially limited by R3, allowing the capacitor in the motor controller to be charged gradually. After a certain period, the delay circuit activates the coil in the contactor, allowing more current to flow into the motor controller through the contactor without damaging the contact points in the contactor.

Following the same concept described, the circuit diagram presented may vary depending on the application. Depending on the specifications of the contactor and the type of load, the electronic components may have different values or configurations.

Besides the switches, there is an energy monitoring device to monitor the voltage and the current. The energy monitoring device is interfaced with an Arduino microcontroller. The Arduino shall relay the voltage and current information to an Android tablet. An Android apps installed in a tablet shall present the data and at the same time it shall do logging on the voltage and the current data. This shall be covered further in the Electronics Dashboard section. Fig. 19 shows the energy monitoring device.

Other than those electronics components, a step-down DC-DC converter is also available for auxiliary power. This shall be used to power the 12V components such as the lights, wipers, horn and other 12V accessories.

4.4. Mechanical Design and Integration

Several steps were taken for mechanical work. The first step involved in removing the ICE components, fuel tank and associated mechanical parts from the diesel tractor. For this conversion project, the original transmission was used. Fig. 20 shows the removed ICE.

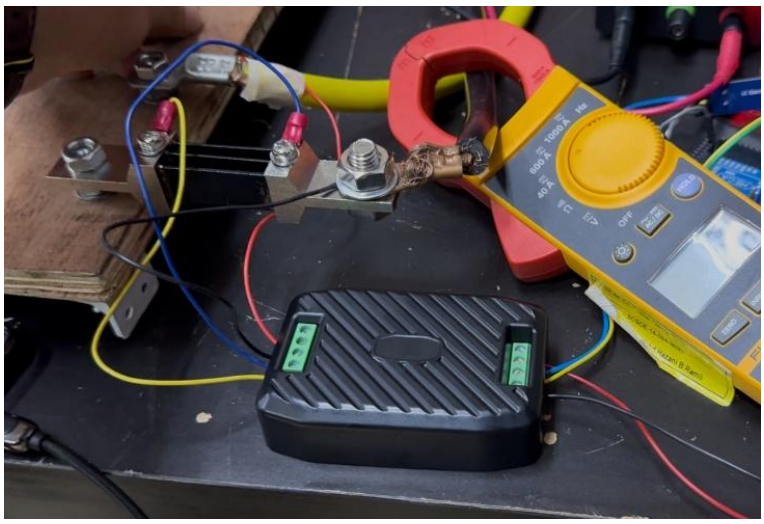

Fig. 19. The energy monitoring device with a shunt resistor

Fig. 20. The ICE of the tractor

4.4.1. Design and Analysis

The next step involved was to create a CAD design for a front chassis structure, a coupler and a mounting frame for the electric motor. The chassis structure serves multiple functions, including housing the battery pack compartment, supporting the tractor's front chassis, and accommodating the electric motor and electronic components. Using factory supplied measurements of the battery cells and electric motor, the design team developed a detailed CAD model for the chassis structure. This allowed the team to virtually assemble and test the components before the actual conversion process. Fig. 21 is the CAD render of the front chassis structure.

As can be observed on Fig. 20, the chassis structure has a compartment for the battery pack on top and the electric motor underneath it. There is also some space for electronics components in front of the electric motor. This design optimizes the tractor’s weight distribution and balance. Efforts were made to achieve the best weight distribution, however there are some restrictions. Due to space limitation, the battery pack compartment was put on top of the electric motor. The weight of the

structure was also considered. Some conversion projects demonstrate that the vehicle is heavier after conversion [67].

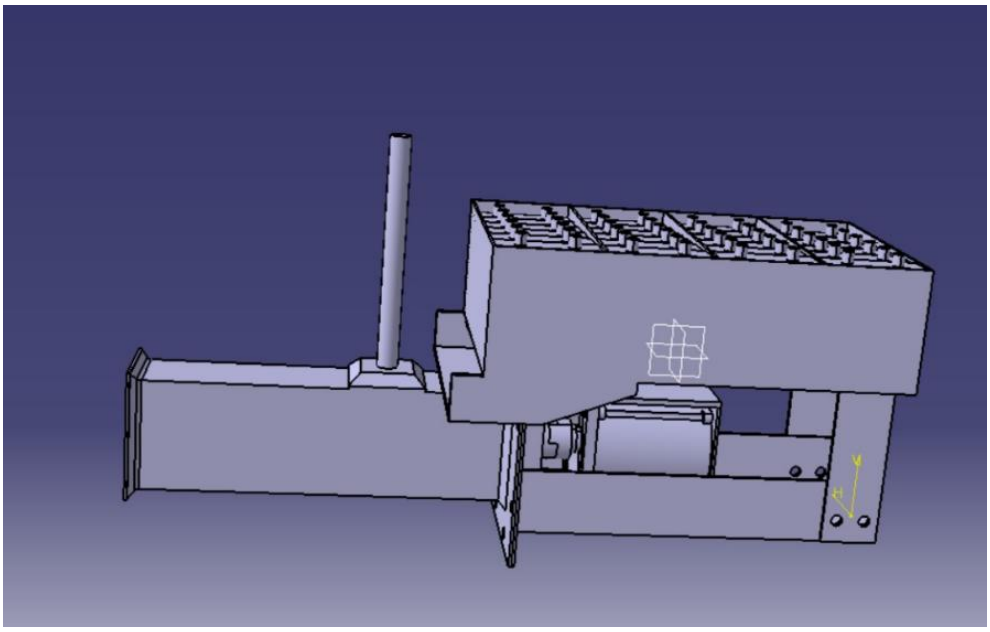

Fig. 21. A CAD render of the front structure of the tractor

The design also considered the accessibility and serviceability of the components for future maintenance. Using the measurements of the battery cells and electric motor dimensions, a mock-up made of cardboard and wood was created. Fig. 22 shows a picture of the mock-up.

Fig. 22. Mock-up components of the tractor

A structural analysis by the design team using Finite Element Analysis (FEA) was performed to ensure the frame can withstand the maximum load of the components and the maximum torque load from the electric motor [68]. A detailed analysis is elaborated in the next section. The results showed that the structure design was adequate and would not fail under the expected operational loads. Another analysis that can be done for further study is on noise and vibration of the PMSM motor. A study suggested using simplified analytical models that can help estimate noise and vibration emissions [69].

Besides the chassis structure, other mechanical components that have been designed were a coupler and a plate for the electric motor mounting. A coupler was designed to connect the electric motor to the existing transmission. A plate for the electric motor mounting was also designed and has been ensured that the mounting is able to hold the electric motor during operation.

4.4.2. EORV Chassis Structural Analysis

A static structural analysis of the EORV was conducted by researchers from the Faculty of Mechanical Technology and Engineering using the finite element method (FEM) in CATIA V5 R20 software under operational loading conditions. The analysis procedure involved defining the material properties, specifying the load and boundary conditions, meshing the geometric model, and evaluating the structural performance through static load analysis. This process aimed to determine the maximum stress and deformation magnitudes, their distribution across the structure, and the overall design safety.

The chassis material selected is low carbon steel (ASTM A36 grade), characterized by a yield strength of 250 MPa, a Young's modulus of 200 GPa, a Poisson's ratio of 0.266, and a density of 7860 kg/m³. Table 6 shows two different loads (force 1 and force 2) applied at the chassis structure for the analysis.

Table 6. Load calculation

Force 1		Force 2	
Electric Motor	19.6 kg	**Battery**	120 kg
Chassis	13.97 kg	**Battery compartment**	24 kg
		Hood	12 kg
Total	32.97 kg = 323.32 N		156kg = 1529.84 N 1529.84 N

The location for applied load and boundary condition (fix or clamp type) was studied before the analysis happened is shown in Fig. 23 and Fig. 24, respectively. The load was divided into two distinct magnitudes and locations to reflect the actual operating conditions. The force applied to the base chassis originates from the electric motor and the chassis weight, whereas the force applied to the side of the chassis results from the battery pack, battery enclosure, and hood components.

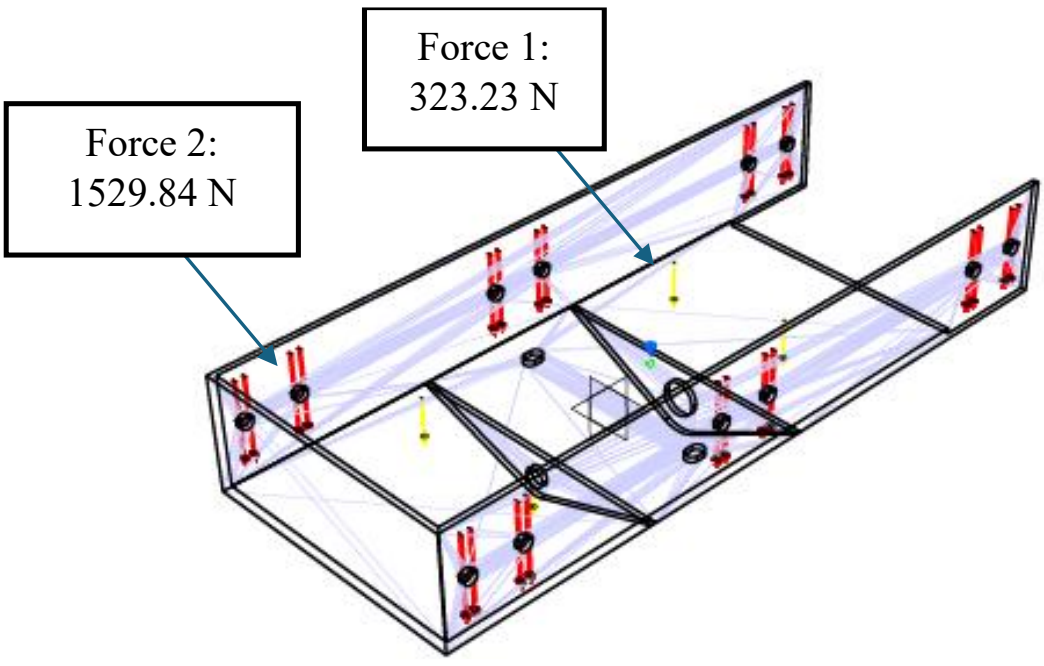

Fig. 23. Applied load location on the chassis

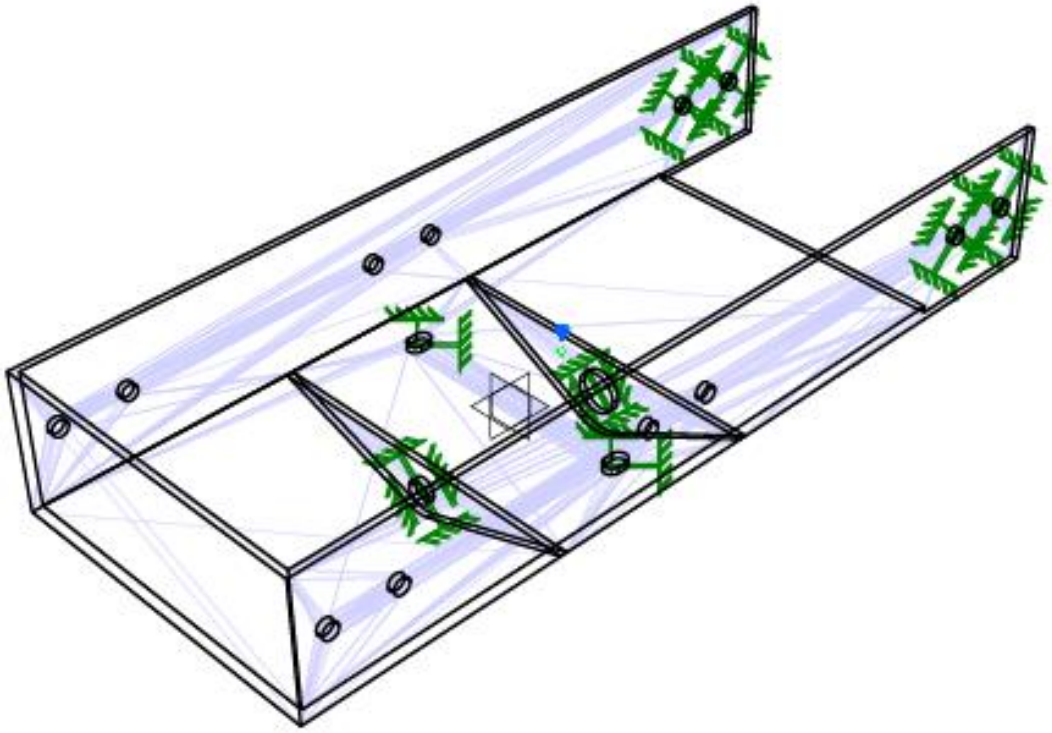

Fig. 24. Boundary condition (fix or clamp type) location

Green colour is the clamp position at the chassis. Clamp was pointed at 8 different locations on the chassis (referring to the mounting points). The meshed model generated is shown in Fig. 25. The meshed model was performed using automatic option, and generated total of 292,301 elements and 1,147,412 nodes, respectively.

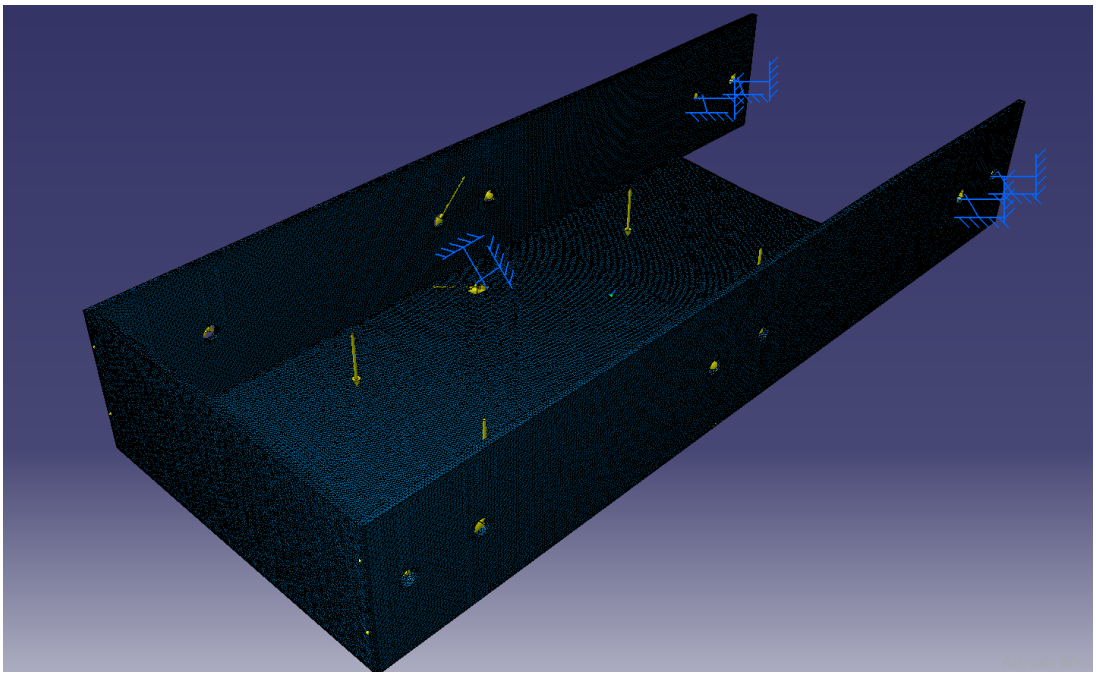

Fig. 25. Meshed model of the EORV chassis

The maximum von Mises stress and stress distribution on the EORV chassis design obtained through the static bending analysis performed is shown in Fig. 26. Meanwhile, the maximum displacement and geometry deformation distribution on the EORV chassis design is shown in Fig. 27.

The maximum bending stress observed was 2.46×107 N/m^2 (or 24.6 MPa) resulting to a Factor of Safety (FOS) under static condition of 10.16. The maximum stress was location observed was at the chassis lower mounting point to the tractor front wheel axle. The high static FOS value obtained showed that the new EORV chassis design is able to robustly withstand the anticipated loads and potential overloads, ensuring the safety and durability of the agricultural machine during its actual operations.

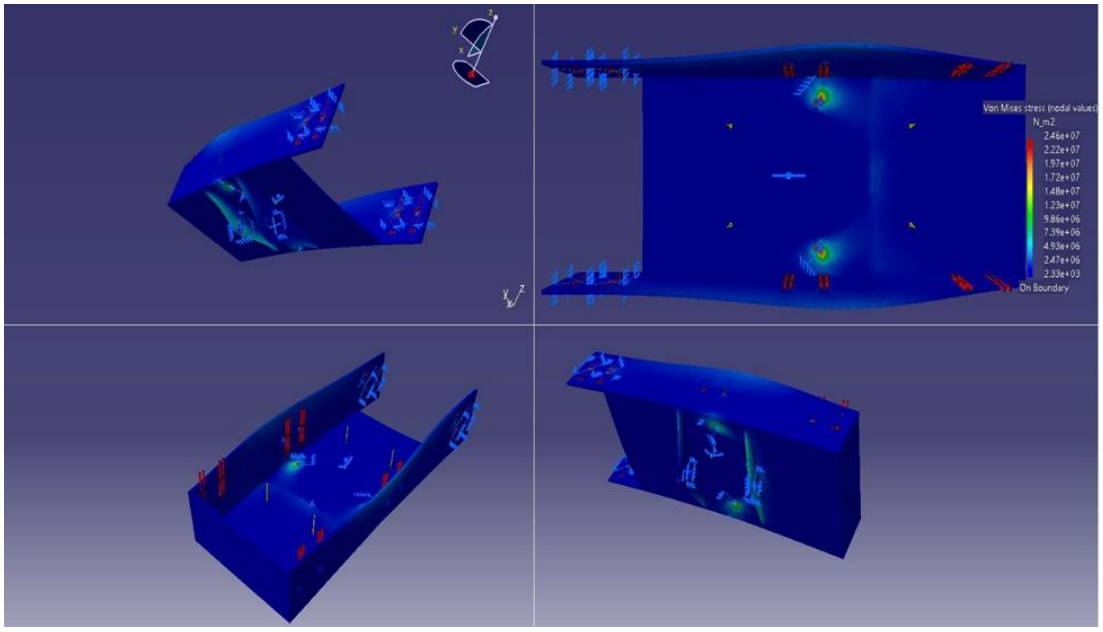

Fig. 26. Bending stress distribution on the E-ORV chassis design at varying view angle

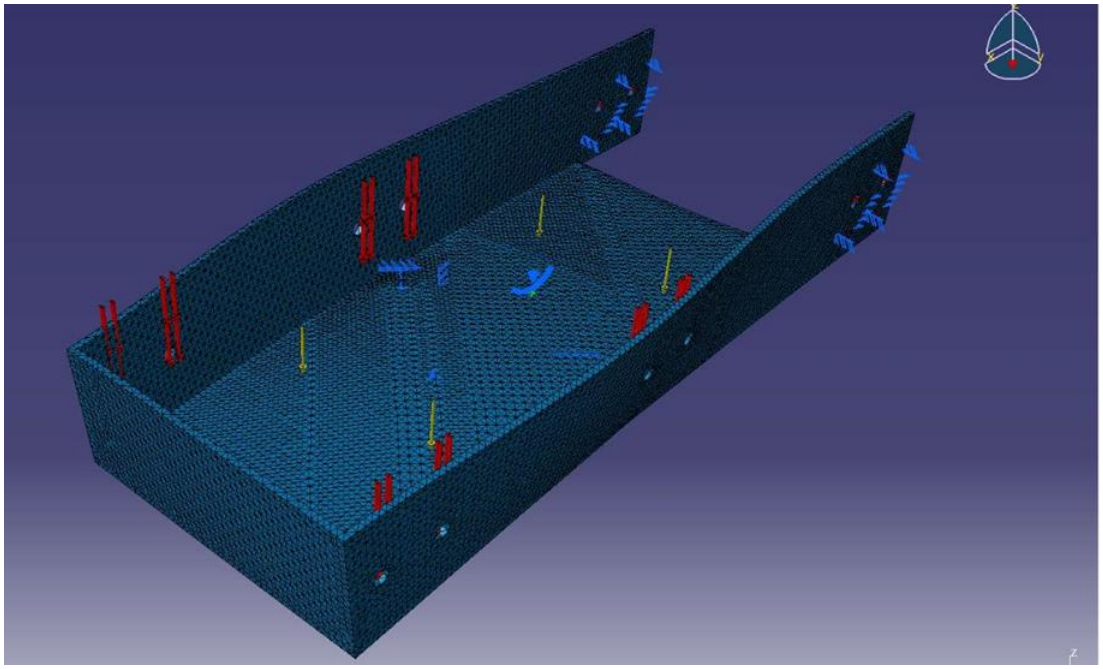

Fig. 27. Displacement distribution on the E-ORV chassis design due to the bending load

4.4.3. Fabrication

There were three main components that need to be fabricated. A chassis structure that has a battery compartment that also houses all electronics component inside, a coupler to couple the electric motor to the transmission and a bracket to hold the electric motor. For this conversion project, the

clutch system was removed, and a coupler was fabricated to directly couple the electric motor to the transmission.

The chassis structure was fabricated using low carbon steel (ASTM grade A36) and was designed to fit the original engine location of the tractor. It was constructed to provide adequate support and protection for the battery cells and other electronic components. Fig. 28 shows the front part of the tractor with the engine removed. Special attention needs to be given to the fact that the removed diesel engine was an integral part of the chassis. The diesel engine was part of the front chassis that also holds the front tyres and axle. Based on the structural analysis, the chassis is expected to withstand all operational loads with an adequate safety margin to accommodate additional forces that may arise during real-world operation. Fig. 29, Fig. 30 & Fig. 31 shows the front structure that holds the front chassis that also houses electronics components underneath it.

Fig. 28. Front part of the chassis without the engine

Fig. 29. Lower part of the customized structure of the tractor

Fig. 30. The customized structure of the tractor

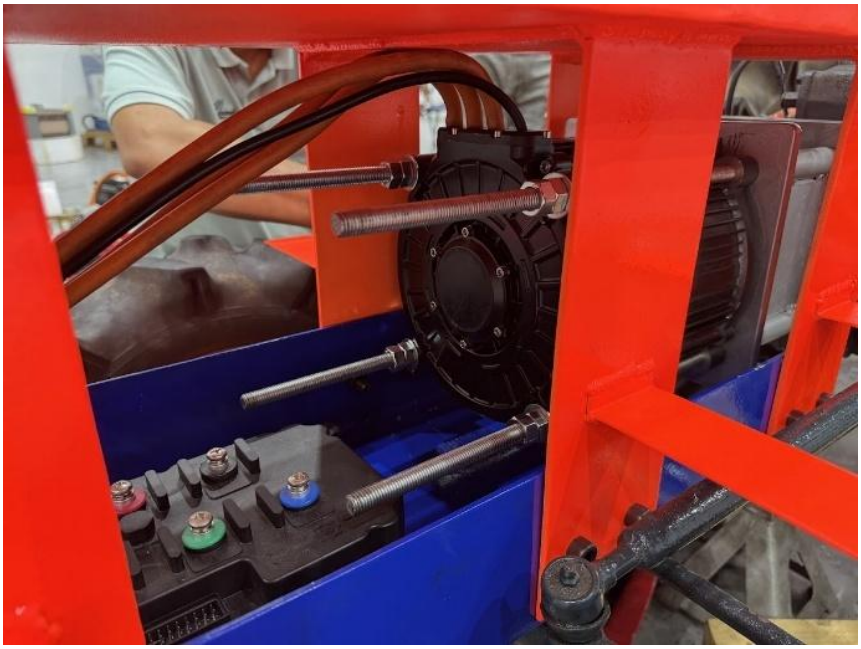

Fig. 31. Electric motor and motor controller underneath the structure

To drive the existing transmission, a coupler was designed and fabricated. The coupler links the electric motor to the transmission. Several types of couplers were designed. For this conversion, a coupler with a flexible jaw design was chosen. The coupler uses a flange, mounted on the electric motor shaft and a matching flange on the input shaft of the transmission, allowing a secure connection between the electric motor and the transmission. Fig. 32 shows the fabricated coupler.

Additionally, a support bracket was designed and fabricated to hold and mount the electric motor to the chassis as in Fig. 33. The bracket was fabricated from steel and was designed to withstand the high torque loads from the electric motor. The electric motor must be aligned properly with the transmission input shaft to avoid any vibration, binding, or premature wear. A precise bracket was fabricated to mount the electric motor in the proper position.

Fig. 32. The flexible jaw coupler with a 3D printed support bracket

Fig. 33. Support bracket for the electric motor mount and the coupler

4.5. Electrical and Electronics Integration

Electrical and electronics integration involved wiring the battery pack, motor controller, electric motor and other electronics components. Before doing the integration, all EV components were bench tested and verified as shown in Fig. 34. This bench test was conducted to ensure that all components are working.

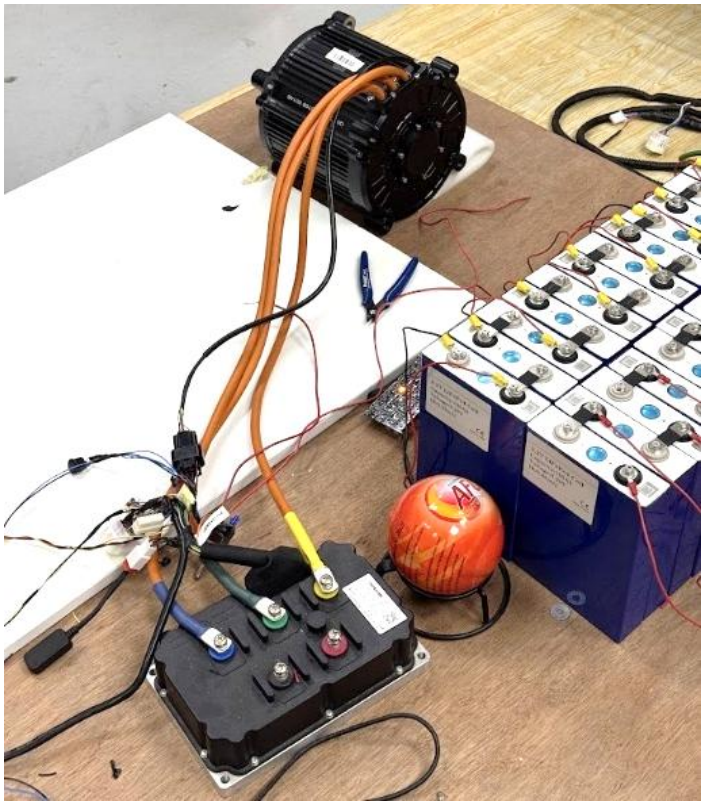

Fig. 34. Bench test of EV components

Prior to installing it into the tractor, each of the battery cells was verified to be balanced and has similar state-of-charge (SoC). The BMS was installed to monitor and manage the battery pack. The BMS includes dedicated software that can be monitored via a mobile phone.

4.5.1. Battery and BMS Integration

As discussed in earlier section, 24 battery cells were connected in series. Each of the battery cells were connected using the supplied bus bar. Each of the battery cell terminals have wire probes from the BMS. Caution was taken to ensure that there is no untoward incident during wiring. From these wire probes, BMS will be monitoring each of the cell's voltage. On top of monitoring function, the BMS can regulate current and provide safety for the battery cells.

There are several effects associated with imbalanced battery cells. J. Oh *et al*. conducted a comprehensive study on the impact of cell imbalance [70]. When cells are imbalanced, voltage variations occur among the cells, accelerating the degradation rate of individual cells. This degradation reduces capacity retention over multiple cycles. Additionally, cell imbalance can lead to an increase in overall internal resistance. From a thermal perspective, voltage imbalance results in uneven discharge patterns, which may generate excess heat and potentially lead to thermal runaway. Charging also poses risks as a battery pack may reach its voltage cutoff indicating a full charge. However, one or more cells may exceed the voltage limit due to imbalance, while others still have remaining capacity. Similarly, during discharge, an imbalanced cell may drop its minimum voltage threshold. These risks, however, can be mitigated by a BMS.

Other issues on the battery pack are the thermal performance of the battery cells. For this EORV, there is no thermal cooling is used. A simple passive cooling methods using fan can be used for further testing. At this stage, there is no endurance test to be done. However, the BMS is used to monitor and to ensure that the temperature is maintained.

Thermal performance of the battery cells represents another area of concern for the battery pack. In the current EORV configuration, no active thermal management system has been implemented.

However, simple passive cooling methods, such as the addition of fans, may be explored in future testing phases. At this stage, endurance testing has not yet been conducted. Nonetheless, the BMS continuously monitors the battery temperature to ensure it remains within safe operating limits.

The BMS comes with a dedicated software that allows the user to monitor the battery pack status and health. There are some parameters that can be configured based on the tractor application. This feature is a bit like the motor controller mentioned in the earlier section. Fig. 35 shows the BMS software.

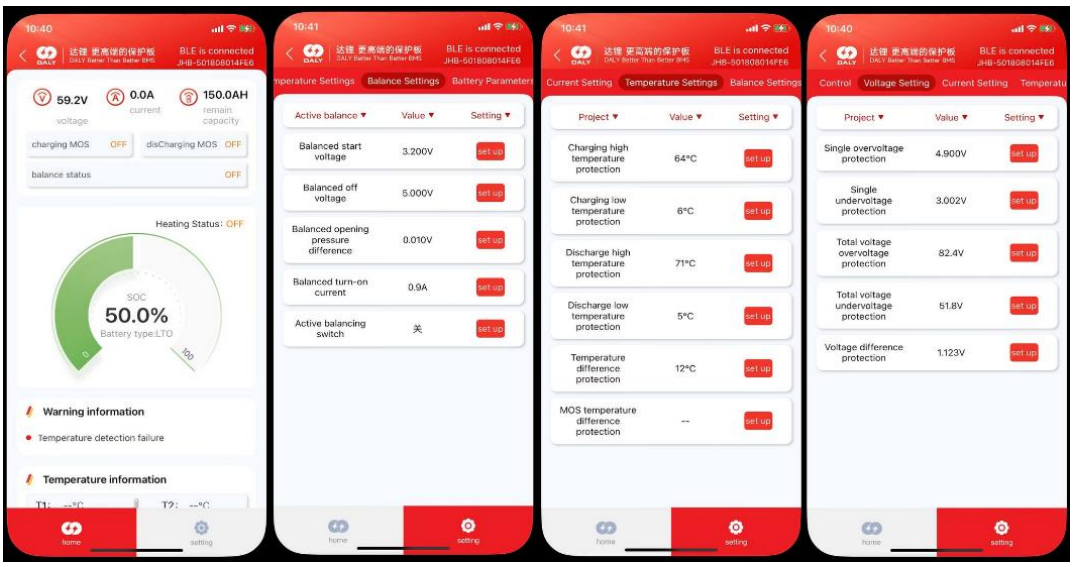

Fig. 35. A snapshot of the BMS software

4.5.2. Pre-Charge and Contactor Circuit

Before connecting the motor controller to the battery pack, the pre-charge circuit shall also be tested here. This is to avoid in-rush current from the battery to the capacitor inside the motor controller. The in-rush current can cause sparks on the battery terminal or on the motor controller terminal when connecting the first time.

The pre-charge circuit in Fig. 18 is referred. A 5-second time delay was setup from the circuit to drive the contactor. The time delay can be chosen as desired. Some analysis was done for this to find a suitable pre-charge resistor. Given that the battery pack maximum voltage is 87.6V, the time to contactor activation is 5s and the measured capacitance across the motor controller is 10.97mF (see Fig. 36), the pre-charge resistor can be calculated.

Assuming that the voltage across the capacitance is 99.5% of the maximum battery voltage just before the contactor is activated, the pre charge can be calculated as follows,

$$V(t) = V_{max}(1 - e^{-t(R \cdot C)})$$

$$V_{max}\ is\ 87.6\ V$$

The voltage just before the contactor is activated will be $V(t)$.

$$V(t)\ is\ 99.5\%\ of\ V_{max}$$

$$0.995\ x\ 87.6V = 87.6V(1 - e^{-5(R \cdot 0.01097)})$$

$$0.995 = 1 - e^{-5(R \cdot 0.01097)}$$

$$e^{-5(R \cdot 0.01097)} = 0.005$$

$$-5/(R \cdot 0.01097) = ln(0.005)$$

$$R = -5/(ln(0.005) \times 0.01097)$$

$= 86.03\ \Omega$

The power rating of the resistor can be calculated as follows,

$$P = \frac{V^2}{R}$$

$$P = \frac{87.6\ V^2}{86.03\ \Omega}$$

$$P = 89.2\ W$$

From the calculations, the pre-charge resistor shall be 86.03 Ω and the power rating is 89.2 W. However, this rating is not available. The closest would be a 100 Ω with 100 W rating. With the new resistor values and the same time delay, the power dissipation and the voltage before contactor activation are calculated. Using the same equation of voltage across the capacitor after 5 seconds with 100Ω.

$$V(t) = V_{max}(1 - e^{-t(R \cdot C)})$$

$$V(t) = 87.6 * (1 - e^{-5(100 \cdot 0.01097)})$$

$$V(t) = 86.67\ V$$

This is about 98.95% of the battery pack voltage

Using the following formula to calculate power dissipation in the resistor

$$P = \frac{V^2}{R}$$

$$P = \frac{87.6^2}{100}$$

$$P = 76.74\ W$$

From the calculation, the 100 Ω with 100 W rating is suitable for this application. It shall be noted that, the calculated power is peak power and when the capacitor is charged, the power will be less. In case of the contactor failure, the pre-charge resistor won't get hot. The potential difference between 86.67 V to 87.6 V is small for spark to occur when the contactor is activated.

4.5.3. Motor Controller

For motor controller, all required sensors and the PMSM were wired and connected to the motor controller. Once those connections were connected, the motor controller was ready to be connected to the pre-charge circuit to the battery pack.

Upon switching it on, the motor controller shall start to operate when the contactor is activated. The motor controller shall give a short tone to indicate that it is ready to operate. Different manufacturers may employ different methods of notification.

Using the software provided by the manufacturer, all parameters can be monitored and some of the parameters can be set [71]. For safety settings, the following can be set, battery pack voltage limit, electric motor or controller temperature limit, electric motor current limit and sensor error. The motor controller will stop working and will produce error when those limits are exceeded or out of range.

For performance settings, the following can be set, maximum electric motor RPM, maximum electric motor torque, throttle curve and regenerative braking. Some of these parameters were tested on bench such as maximum electric motor RPM. Some of them can only be tested with load. This shall be done once the electric motor is installed in the tractor. One parameter that is of interest is the peak current. This can only be tested on the road [72]. Fig. 37 shows the software of the motor controller.

Fig. 36. Measured capacitance across the motor controller

For the bench test, several tests were done to ensure that the throttle is responsive. Settings for RPM limit, motor direction and warning parameters were set. Electric motor failure warning such as low voltage was also simulated. All these steps were taken to ensure proper integration and testing of the electrical system before final installation on the tractor.

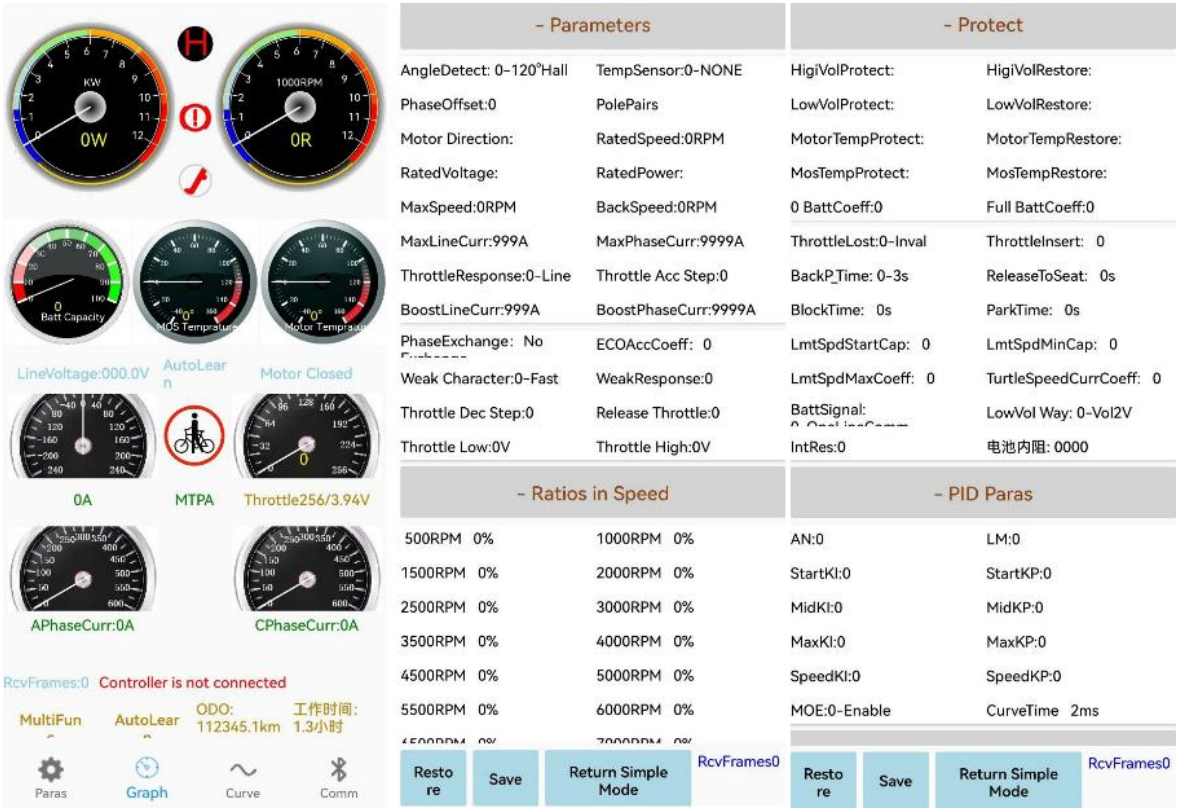

Fig. 37. A snapshot of the motor controller software

4.6. Electronic Dashboard

For this conversion project, there is an electronic dashboard. The electronic dashboard is based on an Android application to display general information of the electric motor like RPM, vehicle

speed, battery voltage, current and power. This information comes from the motor controller and energy monitoring device mentioned earlier. An Arduino microcontroller in Fig. 38 was programmed to capture the sensor data from the motor controller and from the energy monitoring device. The sensor data is transmitted to the tablet through the USB port. Fig. 39 shows the block diagram of the electronics dashboard integration. Fig. 40 shows the interface on the electronics dashboard.

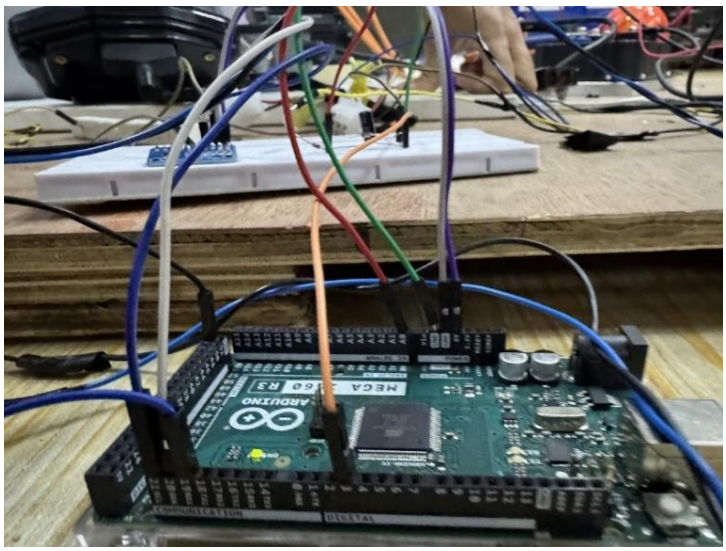

Fig. 38. An Arduino Mega that is used as sensor data collector

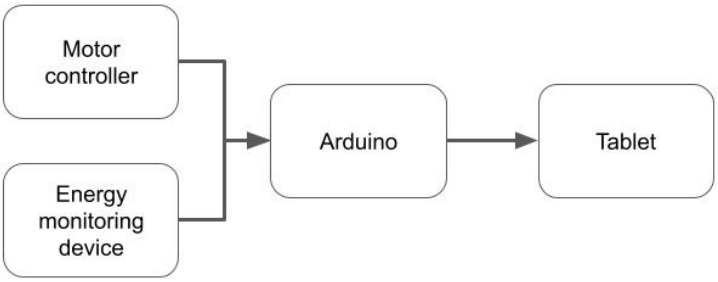

Fig. 39. Block diagram of electronics dashboard

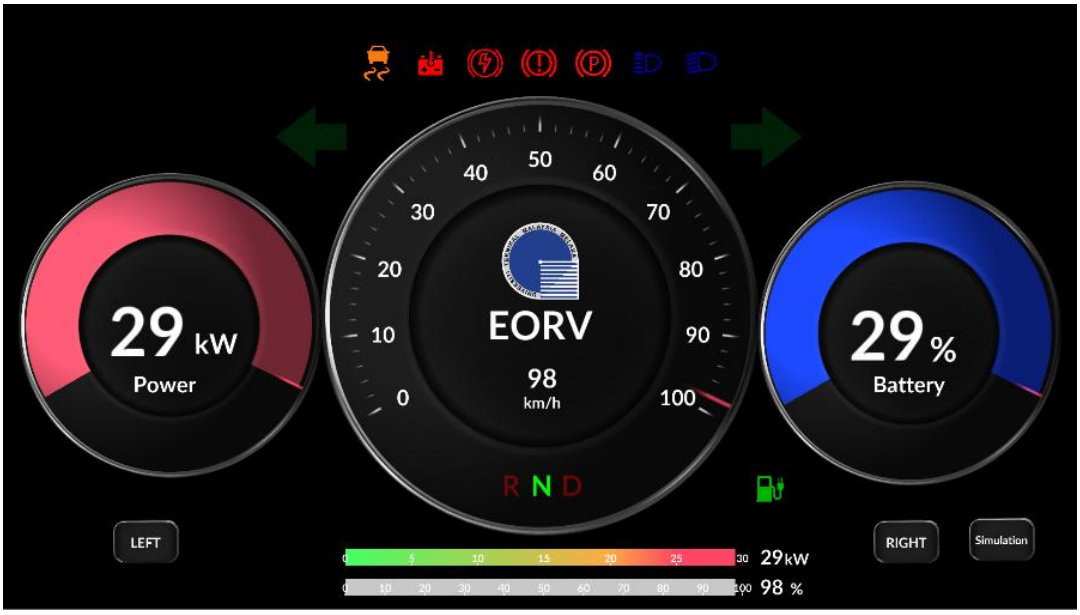

Fig. 40. Interface of the electronics dashboard

5. Performance Evaluation

After completing all installations and integrations, the next step was to evaluate the performance of the EORV. Bench testing has been done before where all electrical and electronics components were tested on a bench. Nevertheless, that was only a small portion of the testing procedures. For this EORV, a simple road test evaluation was conducted.

Before the road test, the tractor was configured and verified in the workshop. When the whole system was good, the tractor was driven out for road tests. For road tests, there was some test runs to capture data. The test plan is described in detail in the next sections.

5.1. Initial Testing

When the tractor was fully assembled, initial testing was conducted to ensure the proper functioning of all the components. At all times, the tractor was suspended on a jack so that the wheels don't touch the ground.

After checking the system, all switches were turned on. Some observations were made to ensure that there was no alarm sound from the motor controller and the BMS indicates normal operation. Then, the tractor will be ready for its initial test. While suspended, a forward gear was shifted in, and the throttle was lightly pressed. From observation, the electric motor started spinning and the traction wheels started to rotate. The test was repeated with other forward and reverse gears. The gear can only be changed when the electric motor is at a complete stop since the clutch has been removed. At the same time, the brake was also tested. When all these have been tested, the tractor was lowered down to the ground.

5.2. Road Test

Once placed on the ground, the tractor underwent a basic road test, as shown in Fig. 41. For this road test, the tractor was driven in a private area where there is no traffic. The tractor was driven slowly and gradually up to speed. Some motor tuning was done to ensure the smoothness of the operation. This is necessary prior to do the test runs.

Fig. 41. The tractor ready to do road test

There were several test runs done for data collection. These test runs were data logged using the combination of Arduino and Android app in the tablet. The recorded data was the voltage of the battery pack, the motor current and the GPS speed. The objective of this test is to investigate motor performance, battery performance and tractor behaviour. The speed of the motor was set to limit of 4500 RPM. The distance of the test is 50 m with some space for slowing down. Fig. 42 shows the test area of the tractor. The tractor can be seen in the background. The stand on the left is a marker that marks 50 m distance from where the tractor starts. The operator shall slow down after reaching the marker.

Fig. 42. The tractor is ready to do a speed run

From a standstill, the operator rapidly depresses the throttle to its maximum position until the tractor reaches terminal speed. The throttle shall remain fully engaged until the tractor reaches the end marker. This ensures that the motor operates at its maximum RPM.

During acceleration from standstill, the current is expected to increase and peak before decreasing once the motor reaches a steady velocity at 4500 RPM. A voltage dip may occur during the current spike. From these two variables, the motor power can be calculated.

6. Test Results

Observations indicated that the tractor has sufficient torque during startup. There was a strong jerk and a slight wheel spinning when the tractor started to move as the torque was being applied instantly. To improve the smoothness of the tractor, the torque curve was adjusted in the motor controller software. From the adjustment, the torque has been reduced slightly. One thing to note is that the initial torque is powerful that the tractor can start with the third gear. Early results show that the tractor has plenty of power with good drivability.

With improved tuning of the motor controller, the tractor was tested in a series of speed runs. A total of five speed runs were conducted. Fig. 43 shows a snapshot of raw data from one of the test runs. The type of recorded data can be seen in the first column of the spreadsheet. Five parameters were recorded: time since data logging started, GPS data, battery voltage, motor current, and power. The time and GPS data were obtained from the internal sensors of the Android tablet. The battery voltage and motor current were acquired from the Arduino that is interfaced with the energy monitoring device. The Arduino relayed the information to the Android tablet via a USB cable.

Time	GPS Altitude	GPS Connected	GPS Date	GPS Heading	GPS Latitude	GPS Longitude	GPS Speed	GPS Time	Voltage (V)	Current (A)	Power (kW)
5.57	42.490173	1	03/21/2025	10.505803	2.318126	102.320915	5.11	10:09 AM	76.27	22.54	1.72
5.69	42.490173	1	03/21/2025	10.505803	2.318126	102.320915	5.11	10:09 AM	75.69	22.54	1.71
5.80	42.490173	1	03/21/2025	10.505803	2.318126	102.320915	5.11	10:09 AM	75.69	22.54	1.71
5.91	42.490173	1	03/21/2025	10.505803	2.318126	102.320915	5.11	10:09 AM	75.69	31.63	2.39
6.02	42.490173	1	03/21/2025	10.505803	2.318126	102.320915	5.11	10:09 AM	75.69	31.63	2.39
6.13	42.233704	1	03/21/2025	10.505803	2.318108	102.320908	8.28	10:09 AM	75.69	31.63	2.39
6.24	42.233704	1	03/21/2025	10.505803	2.318108	102.320908	8.28	10:09 AM	74.09	31.63	2.34
6.35	42.233704	1	03/21/2025	10.505803	2.318108	102.320908	8.28	10:09 AM	74.09	31.63	2.34
6.46	42.233704	1	03/21/2025	10.505803	2.318108	102.320908	8.28	10:09 AM	74.09	102.41	7.59
6.58	42.233704	1	03/21/2025	10.505803	2.318108	102.320908	8.28	10:09 AM	74.09	102.41	7.59
6.69	42.233704	1	03/21/2025	10.505803	2.318108	102.320908	8.28	10:09 AM	74.09	102.41	7.59
6.80	42.233704	1	03/21/2025	10.505803	2.318108	102.320908	8.28	10:09 AM	74.09	102.41	7.59
6.91	42.233704	1	03/21/2025	10.505803	2.318108	102.320908	8.28	10:09 AM	74.09	102.41	7.59
7.02	42.233704	1	03/21/2025	10.505803	2.318108	102.320908	8.28	10:09 AM	67.45	201.95	13.62
7.13	41.345215	1	03/21/2025	10.505803	2.318083	102.320908	15.12	10:09 AM	67.45	201.95	13.62
7.25	41.345215	1	03/21/2025	10.505803	2.318083	102.320908	15.12	10:09 AM	67.45	201.95	13.62
7.36	41.345215	1	03/21/2025	10.505803	2.318083	102.320908	15.12	10:09 AM	67.45	201.95	13.62
7.47	41.345215	1	03/21/2025	10.505803	2.318083	102.320908	15.12	10:09 AM	66.70	98.72	6.58
7.58	41.345215	1	03/21/2025	10.505803	2.318083	102.320908	15.12	10:09 AM	66.70	98.72	6.58
7.69	41.345215	1	03/21/2025	10.505803	2.318083	102.320908	15.12	10:09 AM	66.70	98.72	6.58
7.80	41.345215	1	03/21/2025	10.505803	2.318083	102.320908	15.12	10:09 AM	66.70	98.72	6.58
7.91	41.345215	1	03/21/2025	10.505803	2.318083	102.320908	15.12	10:09 AM	66.70	98.72	6.58
8.03	41.345215	1	03/21/2025	10.505803	2.318083	102.320908	15.12	10:09 AM	72.43	98.72	7.15
8.14	40.510498	1	03/21/2025	188.719467	2.318044	102.320908	18.68	10:09 AM	72.43	98.72	7.15

Fig. 43. A snapshot of speed run #1

Based on the data logs, graphs representing the speed runs were generated. Fig. 44, Fig. 45, Fig. 46, Fig. 47, Fig. 48 show the combined data plots for each respective speed run. From the graphs, several findings aligned with the expected results. A current surge is observed during acceleration, accompanied by a voltage drop. This voltage drop is commonly referred to as a voltage sag.

Despite the manufacturer's 8 kW rating, it can be observed that the motor can deliver higher output for short periods. Speed run #4 recorded the highest current usage. During the speed run, the data log shows that the power peaked at 15.42 kW, with a maximum current of 216.96 A. Fig. 49 presents a snapshot of speed run #4. From the snapshot, approximately 5 seconds into the data log, the current spiked to 216.96 A, accompanied by a voltage sag, where the voltage dropped to 62.34 V. This moment of current spike corresponds to the instance when maximum power was recorded.

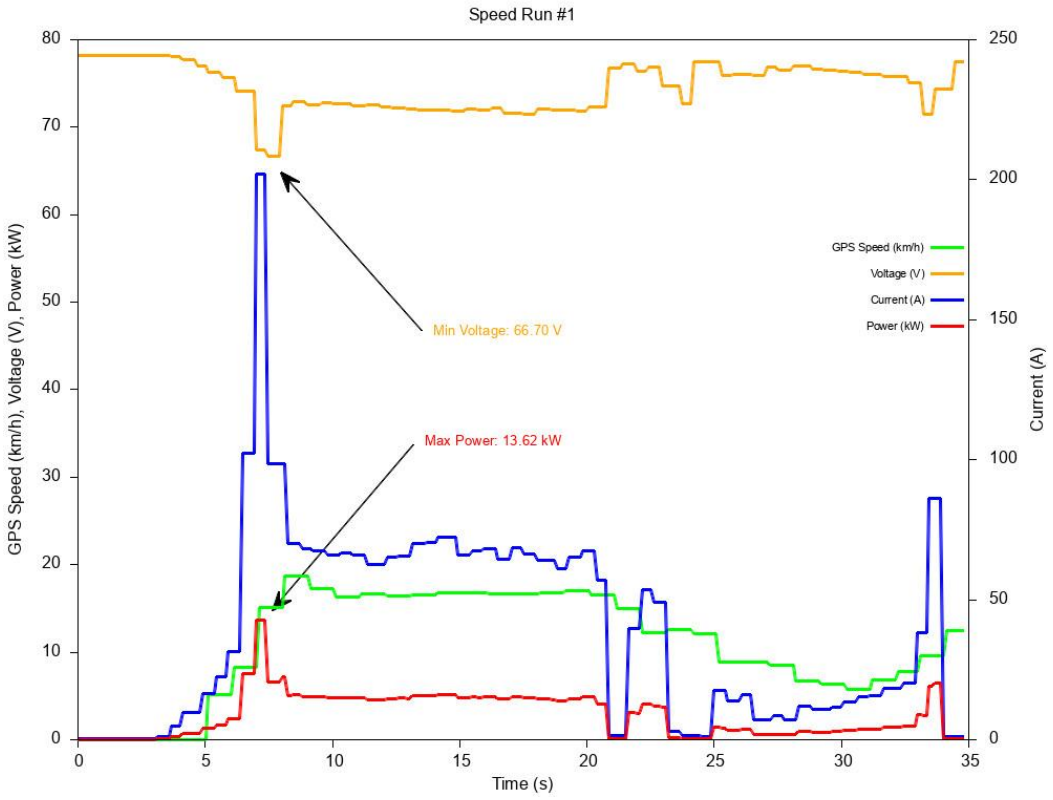

Fig. 44. Speed run #1

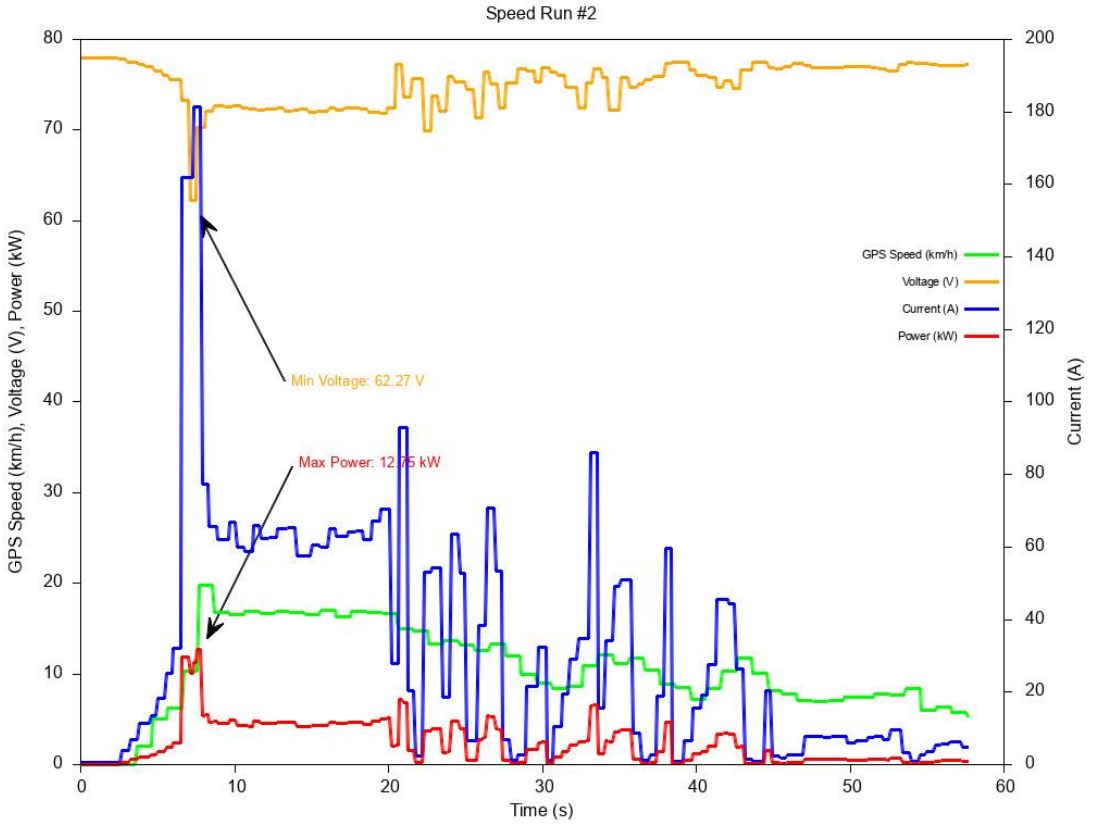

Fig. 45. Speed run #2

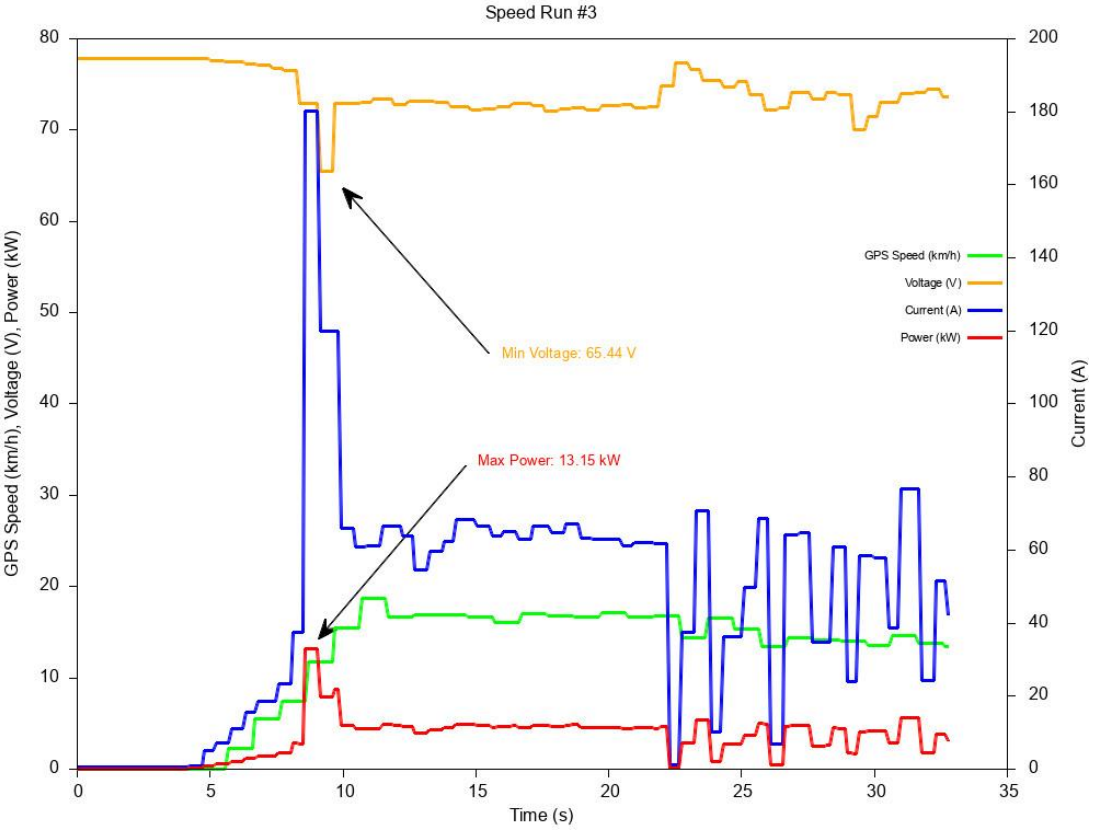

Fig. 46. Speed run #3

International Journal of Robotics and Control Systems
Vol. 5, No. 2, 2025, pp. 1374-1421
ISSN 2775-2658

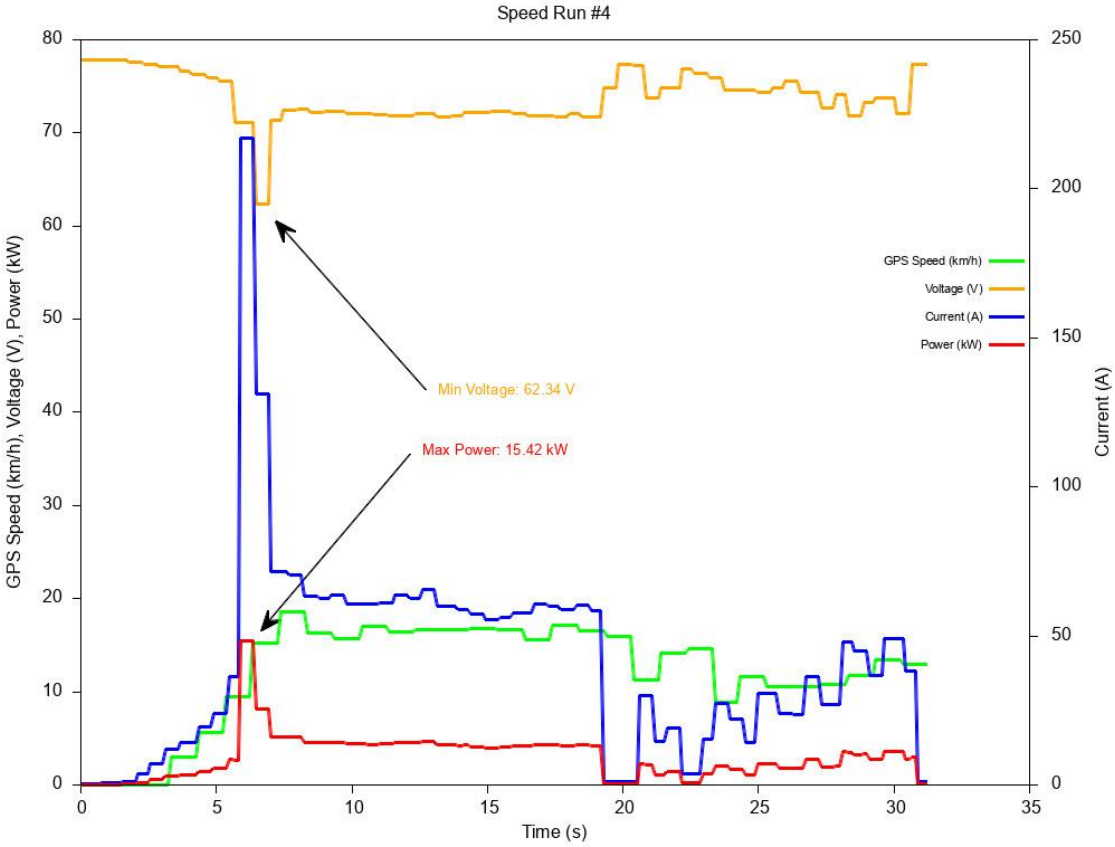

Fig. 47. Speed run #4

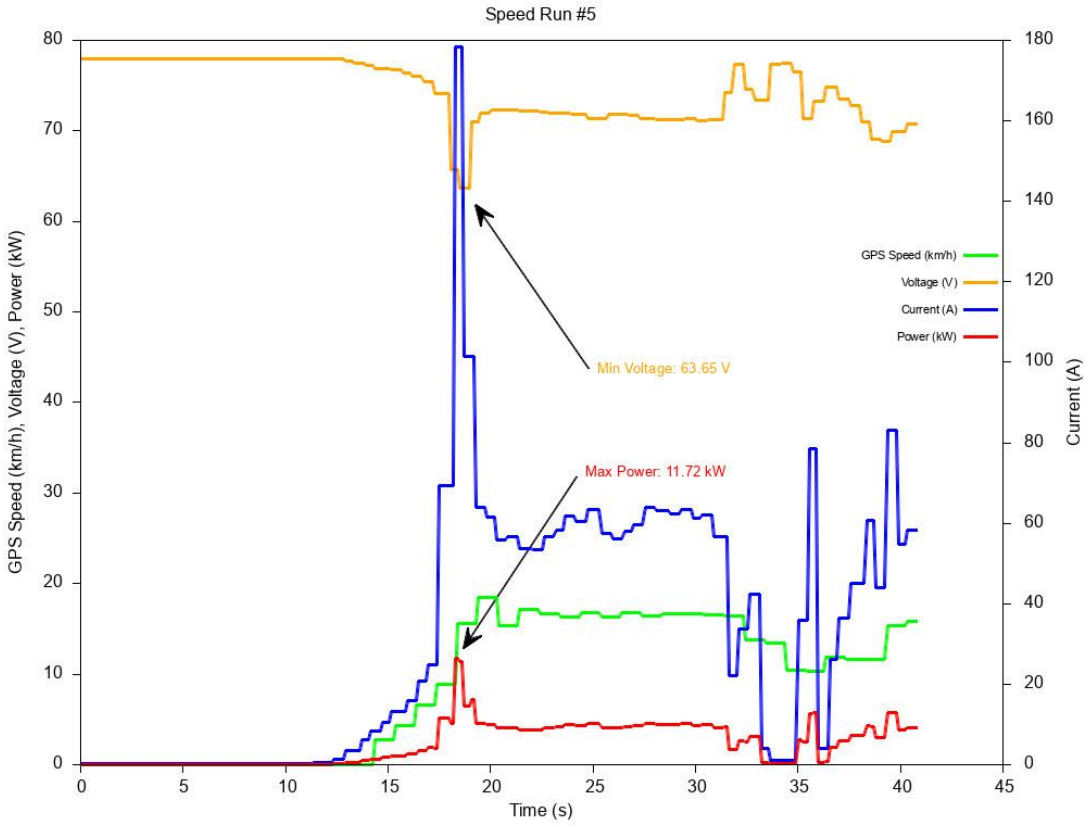

Fig. 48. Speed run #5

Time	GPS Altitude	GPS Connected	GPS Date	GPS Heading	GPS Latitude	GPS Longitude	GPS Speed	GPS Time	Voltage (V)	Current (A)	Power (kW)
5.02	37.984924	1	03/21/2025	6.6728	2.318152	102.320915	5.69	10:23 AM	75.94	23.91	1.82
5.13	37.984924	1	03/21/2025	6.6728	2.318152	102.320915	5.69	10:23 AM	75.52	23.91	1.81
5.24	37.984924	1	03/21/2025	6.6728	2.318152	102.320915	5.69	10:23 AM	75.52	23.91	1.81
5.35	38.206665	1	03/21/2025	6.6728	2.318132	102.320915	9.43	10:23 AM	75.52	23.91	1.81
5.46	38.206665	1	03/21/2025	6.6728	2.318132	102.320915	9.43	10:23 AM	75.52	36.25	2.74
5.57	38.206665	1	03/21/2025	6.6728	2.318132	102.320915	9.43	10:23 AM	75.52	36.25	2.74
5.69	38.206665	1	03/21/2025	6.6728	2.318132	102.320915	9.43	10:23 AM	71.07	36.25	2.58
5.80	38.206665	1	03/21/2025	6.6728	2.318132	102.320915	9.43	10:23 AM	71.07	36.25	2.58
5.91	38.206665	1	03/21/2025	6.6728	2.318132	102.320915	9.43	10:23 AM	71.07	216.96	15.42
6.02	38.206665	1	03/21/2025	6.6728	2.318132	102.320915	9.43	10:23 AM	71.07	216.96	15.42
6.13	38.206665	1	03/21/2025	6.6728	2.318132	102.320915	9.43	10:23 AM	71.07	216.96	15.42
6.24	38.206665	1	03/21/2025	6.6728	2.318132	102.320915	9.43	10:23 AM	71.07	216.96	15.42
6.36	38.169922	1	03/21/2025	6.6728	2.318099	102.320915	15.26	10:23 AM	71.07	216.96	15.42
6.47	38.169922	1	03/21/2025	6.6728	2.318099	102.320915	15.26	10:23 AM	62.34	131.11	8.17
6.58	38.169922	1	03/21/2025	6.6728	2.318099	102.320915	15.26	10:23 AM	62.34	131.11	8.17
6.69	38.169922	1	03/21/2025	6.6728	2.318099	102.320915	15.26	10:23 AM	62.34	131.11	8.17
6.80	38.169922	1	03/21/2025	6.6728	2.318099	102.320915	15.26	10:23 AM	62.34	131.11	8.17
6.91	38.169922	1	03/21/2025	6.6728	2.318099	102.320915	15.26	10:23 AM	62.34	131.11	8.17
7.02	38.169922	1	03/21/2025	6.6728	2.318099	102.320915	15.26	10:23 AM	71.32	71.53	5.1
7.13	38.169922	1	03/21/2025	6.6728	2.318099	102.320915	15.26	10:23 AM	71.32	71.53	5.1

Fig. 49. Speed run #4

When the motor reaches its speed limit, the current dropped to a steady value. Using the same data from Speed Run #4, between 8.81 seconds and 11.71 seconds, it can be observed that the current stabilizes between 60 A and 63 A, and the power remains steady between 4.3 kW and 4.5 kW. Fig. 50 shows the data log for the specified period. From this speed run result, it can be concluded that at a steady-state speed of 4500 RPM, the motor produces between 4.3 kW and 4.5 kW of power. This indicates that sufficient power is available for higher load conditions.

Time	GPS Altitude	GPS Connected	GPS Date	GPS Heading	GPS Latitude	GPS Longitude	GPS Speed	GPS Time	Voltage (V)	Current (A)	Power (kW)
8.81	38.369995	1	03/21/2025	177.77034	2.318014	102.320923	16.31	10:23 AM	72.25	62.59	4.52
8.92	38.369995	1	03/21/2025	177.77034	2.318014	102.320923	16.31	10:23 AM	72.25	62.59	4.52
9.03	38.369995	1	03/21/2025	177.77034	2.318014	102.320923	16.31	10:23 AM	72.27	62.59	4.52
9.14	38.369995	1	03/21/2025	177.77034	2.318014	102.320923	16.31	10:23 AM	72.27	62.59	4.52
9.25	38.369995	1	03/21/2025	177.77034	2.318014	102.320923	16.31	10:23 AM	72.27	63.75	4.61
9.37	38.796692	1	03/21/2025	179.600464	2.317968	102.320923	15.77	10:23 AM	72.27	63.75	4.61
9.48	38.796692	1	03/21/2025	179.600464	2.317968	102.320923	15.77	10:23 AM	72.27	63.75	4.61
9.59	38.796692	1	03/21/2025	179.600464	2.317968	102.320923	15.77	10:23 AM	72.27	63.75	4.61
9.70	38.796692	1	03/21/2025	179.600464	2.317968	102.320923	15.77	10:23 AM	72.27	63.75	4.61
9.81	38.796692	1	03/21/2025	179.600464	2.317968	102.320923	15.77	10:23 AM	72.09	60.75	4.38
9.92	38.796692	1	03/21/2025	179.600464	2.317968	102.320923	15.77	10:23 AM	72.09	60.75	4.38
10.03	38.796692	1	03/21/2025	179.600464	2.317968	102.320923	15.77	10:23 AM	72.09	60.75	4.38
10.15	38.796692	1	03/21/2025	179.600464	2.317968	102.320923	15.77	10:23 AM	72.09	60.75	4.38
10.26	38.796692	1	03/21/2025	179.600464	2.317968	102.320923	15.77	10:23 AM	72.09	60.75	4.38
10.37	38.396484	1	03/21/2025	179.600464	2.317924	102.320923	16.99	10:23 AM	72.14	60.75	4.38
10.48	38.396484	1	03/21/2025	179.600464	2.317924	102.320923	16.99	10:23 AM	72.14	60.75	4.38
10.59	38.396484	1	03/21/2025	179.600464	2.317924	102.320923	16.99	10:23 AM	72.14	60.56	4.37
10.70	38.396484	1	03/21/2025	179.600464	2.317924	102.320923	16.99	10:23 AM	72.14	60.56	4.37
10.82	38.396484	1	03/21/2025	179.600464	2.317924	102.320923	16.99	10:23 AM	71.91	60.56	4.35
10.93	38.396484	1	03/21/2025	179.600464	2.317924	102.320923	16.99	10:23 AM	71.91	60.56	4.35
11.04	38.396484	1	03/21/2025	179.600464	2.317924	102.320923	16.99	10:23 AM	71.91	61.05	4.39
11.15	38.396484	1	03/21/2025	179.600464	2.317924	102.320923	16.99	10:23 AM	71.91	61.05	4.39
11.26	38.396484	1	03/21/2025	179.600464	2.317924	102.320923	16.99	10:23 AM	71.91	61.05	4.39
11.37	37.886353	1	03/21/2025	177.802872	2.317878	102.320923	16.45	10:23 AM	71.81	61.05	4.38
11.48	37.886353	1	03/21/2025	177.802872	2.317878	102.320923	16.45	10:23 AM	71.81	61.05	4.38
11.60	37.886353	1	03/21/2025	177.802872	2.317878	102.320923	16.45	10:23 AM	71.81	63.72	4.58
11.71	37.886353	1	03/21/2025	177.802872	2.317878	102.320923	16.45	10:23 AM	71.81	63.72	4.58

Fig. 50. Speed run #4 from 8.81 seconds to 11.71 seconds

7. Discussions

From the speed runs, the voltage sag occurs in the early stage of motor acceleration. The voltage sag, also known as voltage dip, is a temporary reduction voltage level in an electrical power supply system. It causes by sudden increase in loads such as motors, water pump and air conditioner. In EVs, high torque demands lead to a sudden draw of high current, causing a temporary voltage drop across the battery or power delivery system. There are several studies and mitigation procedure for this phenomenon.

One study by I. Hermawan *et al*. [73], explored the technique of using photovoltaic (PV) farm to address issues caused by the start-up of large industrial motors. The PV was coupled with

supercapacitors. The simulation done suggest a reduction of voltage sag from 6.71% to under 5% and sag duration from 5.3 seconds to 4.9 seconds.

Another related study by M. Hashem *et al*. [74] proposes the use of superconducting magnetic energy storage (SMES) to reduce voltage sag by simultaneous start-up of water-pumping motors. From a novel method of control strategy of the SMES, the simulated system improved the power system.

In another study on a real power distribution feeder, research was done with supercapacitor. M. Khamies *et al*. [75] proposes the use and the control of supercapacitor energy storage (SCES) instead of SMES. In this study, the SCES has better advantage compared to SMES in mitigating voltage sag in terms of lower energy capacity and cost.

On larger scale, voltage sag can affect public power supply. For example, in China's distribution network on EV charging infrastructure, Y. Zhang *et al*. [76] studied and evaluated voltage sag on EV charging quality. The study emphasizes the significance of understanding voltage sag's effects on electric vehicle charging quality, as insufficient evaluation of voltage sag can hinder EV development. The study found that voltage sag significantly reduces the charging current of EVs and can even lead to short-term interruptions during charging.

In the results, voltage sag is significant. From speed run #4, it can be observed that the peak current occurred between time 5.91 seconds to 6.47 seconds. For 0.56 seconds, the current peaked at 217 A. The voltage dropped between time 6.47 seconds to 7.02 seconds. During this period, the voltage dropped from 75.94 V to 62.34 V before stabilizes between 71V to 72 V in Fig. 50.

The voltage was dropping close to the minimum operational limit of the battery pack. For a 24s configuration, the minimum operational limit is 60 V. Two solutions can be applied. One with supercapacitor and one with better control strategy of the motor controller settings. However, it must be investigated thoroughly before applying the solutions. From the data logs, the battery voltage was slightly below the nominal voltage of 76.8 V. The battery was not fully charged. Before implementing the supercapacitor solution, the normal behaviour of the whole system must be understood. The voltage dipped to 62 V for half a second in the speed run. There are some other uncertainties on how low the voltage will drop when the battery pack is below 70 V. And there shall be some questions if the tractor is pulling a load for a longer period like 10 seconds. For this, a test similar to the drawbar test as discussed in the literature review can be applied for future work.

The results also show that the motor performance has surpassed the original diesel engine in term of torque and power. Based on the available specifications, the rated engine speed is 3000 RPM. During the speed run, the electric motor operated at a maximum speed of 4500 RPM without any issues observed. However, a more comprehensive study of the mechanical components is necessary, as the actual maximum RPM of the original diesel engine remains uncertain. Some unofficial sources describe the typical operating speed of the diesel engine is around 3000 RPM, which is considered the point of optimal efficiency. It is essential to verify this information through empirical testing or official documentation to ensure compatibility and long-term reliability of the drivetrain under increased rotational speeds. Additionally, stress analysis on components such as the gearbox, PTO, and differential should be considered to assess their performance beyond the original design specifications.

8. Further Work

As discussed, there are several areas that can be further explored to enhance the performance of the converted tractor. Addressing current uncertainties is essential to ensure the overall feasibility of the conversion.

In terms of battery performance, preliminary results indicate a significant voltage sag during acceleration. This phenomenon should be evaluated under various battery pack voltages and different load conditions. Detailed analysis is also necessary to better understand the motor's load behaviour. Additionally, the thermal characteristics of the battery pack require further investigation. Although

$LiFePO_4$ cells are known for their superior thermal safety, studying their actual thermal performance under operational conditions may reveal opportunities for improvement and optimization.

Another critical area is motor performance. While initial tests have provided some insights, further experimentation is needed to comprehensively assess the powertrain in terms of power output and energy consumption. A well-structured testing methodology should be developed, with a focus on traction performance and overall energy efficiency. Alongside these efforts, the battery pack design can be optimized, and an in-depth study on accurate state-of-charge (SoC) estimation should be conducted.

While performance evaluation for acceleration and top speed are straightforward, the performance evaluation for endurance and energy consumption are quite challenging. There are standards for passenger vehicles such as New European Driving Cycle (NEDC), Worldwide Harmonized Light Vehicles Test Cycle (WLTP) and Environmental Protection Agency (EPA) [77]. However, for agricultural tractors, these standards are irrelevant.

For agriculture, the tractors are fall under non-road mobile machinery category [78], [79]. To name a few, there are European Stage V, ISO 8178, and OECD Tractor Codes (as mentioned in literature review) [80]-[82]. These standards have been developed by some countries and the international bodies and mostly are for emission testing. There are also some standards that evaluate not only energy consumption but the tractor's attachment performance and safety [83].

9. Conclusion

This paper has presented the process of converting a diesel-powered tractor into an electric model. The design, selection, and integration of major components such as the electric motor, motor controller, battery pack, BMS, and other electronic components were covered in detail. The initial test demonstrates that the converted electric tractor can match the performance of its diesel counterpart in terms of power while providing improved efficiency and lower emissions.

It is noted that greater challenges arise during the conversion process. The estimation of the battery pack is a simplistic one and the battery dimensioning is limited by the size of the tractor and the expected overall weight post-conversion. While software simulation may address some issues, a more suitable method would be field testing with a proper test methodology. A speed run can only evaluate the maximum power of the motor on a flat surface; however, in real-world operation, more variables can affect energy consumption. From the speed run test, an issue with voltage sag was discovered. A further comprehensive testing procedure is likely to reveal further challenges.

The fabricated mechanical components have been simulated in the software. Based on the simulation results, the parts are expected to withstand the forces under load. However, there is uncertainty regarding the original mechanical parts, such as the gear and transmission shaft, when operating above their rated RPM. The fabricated mechanical components should be dismantled and inspected during each test procedure. It is advisable to keep the motor speed below the recommended operating RPM.

As discussed in the literature review, the conversion process can be costly initially. In the long term, however, the cost of maintenance should be lower. The most significant issue is battery degradation. Certain optimizations can be implemented to prolong battery life, including setting limits on both low battery levels and full charge levels. This is to ensure that the battery cells operate at an optimum voltage. Furthermore, operators can be trained to ensure optimal operation that extends battery lifespan.

In this EORV project, the initial cost is relatively high. However, the cost can be minimized if the conversion is carried out on multiple tractors simultaneously rather than on a single unit. Purchasing motors and battery cells in bulk would also reduce the initial investment. As highlighted

in one of the reviewed studies, electric tractor conversion may be further encouraged through government incentives.

With the experience gained from the conversion process and the initial test results, a comprehensive set of test procedures under various operating conditions should be developed. These tests are essential to fully understand the tractor's performance envelope, with a focus on optimizing energy efficiency, improving battery management, and refining drivetrain performance.

Author Contribution: All authors contributed equally to the main contributor to this paper. All authors read and approved the final paper.

Funding: This research received a fund from UTeM's grant with a project number PJP/2023/CeRIA/EV/Y00008.

Acknowledgement: The authors wish to express their gratitude to Faculty of Electrical Technology and Engineering, Universiti Teknikal Malaysia Melaka (UTeM) and all those who provided invaluable assistance throughout this research. The authors also would like to thank System Consultancy Services Sdn Bhd for providing support for this paper.

Conflict of Interest: The authors declare no conflict of interest.

References

[1] I. Veza *et al*., "Electric Vehicles in Malaysia and Indonesia: Opportunities and Challenges," *Energies*, vol. 15, no. 7, p. 2564, 2022, https://doi.org/10.3390/en15072564.

[2] N. A. Q. Muzir, Md. R. H. Mojumder, Md. Hasanuzzaman, and J. Selvaraj, "Challenges of Electric Vehicles and Their Prospects in Malaysia: A Comprehensive Review," *Sustainability*, vol. 14, no. 14, p. 8320, 2022, https://doi.org/10.3390/su14148320.

[3] H. A. Abbasi, Z. H. Shaari, and W. Moughal, "Consumer Motivation to Enhance Purchase Intention Towards Electric Vehicles in Malaysia," *SHS Web of Conferences*, vol. 124, p. 09003, 2021, https://doi.org/10.1051/shsconf/202112409003.

[4] V. Sivasamy, N. Yusoff, and A. Abd-Rahman, "Powering electric cars in Malaysia with green electricity produced from oil palm biomass," *IOP Conference Series: Materials Science and Engineering*, vol. 736, no. 3, p. 032014, 2020, https://doi.org/10.1088/1757-899x/736/3/032014.

[5] C. Clonts, "CNH introduces battery-electric, autonomous-ready tractor," *SAE International*, 2022, https://www.sae.org/news/2022/12/cnh-tech-day-new-tractors.

[6] R. Melo, F. L. M. Antunes, S. Daher, H. H. Vogt, D. Albiero, and F. L. Tofoli, "Conception of an electric propulsion system for a 9 kW electric tractor suitable for family farming," *IET Electric Power Applications*, vol. 13, no. 12, pp. 1993-2004, 2019, https://doi.org/10.1049/iet-epa.2019.0353.

[7] E. S. Gautam and A. Dubey, "Conversion of Hydrocarbon Fueled Based Mini Hand Tractor into Electric Based Hand Mini Tractor," *International Journal for Research in Applied Science and Engineering Technology*, vol. 11, no. 9, pp. 868-871, 2023, https://doi.org/10.22214/ijraset.2023.55745.

[8] Y. Ueka, J. Yamashita, K. Sato, and Y. Doi, "Study on the Development of the Electric Tractor," *Engineering in Agriculture, Environment and Food*, vol. 6, no. 4, pp. 160-164, 2013, https://doi.org/10.11165/eaef.6.160.

[9] K. Plizga, "Analysis of Energy Consumption by Electric Agricultural Tractor Model Under Operating Conditions," *Agricultural Engineering*, vol. 25, no. 1, pp. 1–12, 2021, https://doi.org/10.2478/agriceng-2021-0001.

[10] C. R. Gade and R. S. Wahab, "Conceptual Framework for Modelling of an Electric Tractor and Its Performance Analysis Using a Permanent Magnet Synchronous Motor," *Sustainability*, vol. 15, no. 19, p. 14391, 2023, https://doi.org/10.3390/su151914391.

[11] R. Dhond, U. Srivastav, B. T. Patil, and H. Vaishnav, "Comparative Study of Electric Tractor and Diesel Tractor," *IOP Conference Series: Materials Science and Engineering*, vol. 1168, no. 1, p. 012003, 2021, https://doi.org/10.1088/1757-899x/1168/1/012003.

[12] D. Bessette, D. Brainard, A. Srivastava, W. Lee, and S. Geurkink, "Battery Electric Tractors: Small-Scale Organic Growers' Preferences, Perceptions, and Concerns," *Energies*, vol. 15, no. 22, p. 8648, 2022, https://doi.org/10.3390/en15228648.

[13] H. Gao and J. Xue, "Modeling and economic assessment of electric transformation of agricultural tractors fueled with diesel," *Sustainable Energy Technologies and Assessments*, vol. 39, p. 100697, 2020, https://doi.org/10.1016/j.seta.2020.100697.

[14] Y. Lu and T. Zhu, "Status and prospects of lithium iron phosphate manufacturing in the lithium battery industry," *MRS Communications*, vol. 14, no. 5, pp. 888-899, 2024, https://doi.org/10.1557/s43579-024-00644-2.

[15] Z. Tang *et al*., "Unlocking superior safety, rate capability, and low-temperature performances in LiFePO4 power batteries," *Energy Storage Materials*, vol. 67, p. 103309, 2024, https://doi.org/10.1016/j.ensm.2024.103309.

[16] T. Chen, M. Li, and J. Bae, "Recent Advances in Lithium Iron Phosphate Battery Technology: A Comprehensive Review," *Batteries*, vol. 10, no. 12, p. 424, 2024, https://doi.org/10.3390/batteries10120424.

[17] R. M. C. Amongo, E. P. Quilloy, M. A. F. Ranches, M. V. L. Larona, and M. S. Madlangbayan, "Development of an electric hand tractor (e-Tractor) for agricultural operations," *IOP Conference Series: Earth and Environmental Science*, vol. 542, no. 1, p. 012027, 2020, https://doi.org/10.1088/1755-1315/542/1/012027.

[18] N. Chavan and V. Rathor, "Transition of ICEV to EV: Process and Efficiency," *International Journal of Engineering Applied Sciences and Technology*, vol. 5, no. 3, pp. 402-408, 2020, https://doi.org/10.33564/IJEAST.2020.v05i03.064.

[19] Z. Liu *et al*., "Comparing total cost of ownership of battery electric vehicles and internal combustion engine vehicles," *Energy Policy*, vol. 158, p. 112564, 2021, https://doi.org/10.1016/j.enpol.2021.112564.

[20] D. Kryzia and K. Kryzia, "An evaluation of the potential of the conversion of passenger cars powered by conventional fuels into electric vehicles," *Polityka Energetyczna – Energy Policy Journal*, vol. 26, no. 3, pp. 171-186, 2023, https://doi.org/10.33223/epj/171324.

[21] S. Ahmad, M. Z. A. A. Kadir, and S. Shafie, "Current perspective of the renewable energy development in Malaysia," *Renewable and Sustainable Energy Reviews*, vol. 15, no. 2, pp. 897-904, 2011, https://doi.org/10.1016/j.rser.2010.11.009.

[22] D.-H. Kim, M.-J. Kim, and B.-K. Lee, "An Integrated Battery Charger With High Power Density and Efficiency for Electric Vehicles," *IEEE Transactions on Power Electronics*, vol. 32, no. 6, pp. 4553-4565, 2017, https://doi.org/10.1109/tpel.2016.2604404.

[23] H. V. Nguyen, D.-C. Lee, and F. Blaabjerg, "A Novel SiC-Based Multifunctional Onboard Battery Charger for Plug-In Electric Vehicles," *IEEE Transactions on Power Electronics*, vol. 36, no. 5, pp. 5635-5646, 2021, https://doi.org/10.1109/tpel.2020.3026034.

[24] S.-Y. Lee, W.-S. Lee, J.-Y. Lee, and I.-O. Lee, "High-efficiency 11 kW bi-directional on-board charger for EVs," *Journal of Power Electronics*, vol. 22, no. 2, p. 376, 2022, https://doi.org/10.1007/s43236-021-00344-3.

[25] X. Liu *et al*., "From NEDC to WLTP: Effect on the Energy Consumption, NEV Credits, and Subsidies Policies of PHEV in the Chinese Market," *Sustainability*, vol. 12, no. 14, p. 5747, 2020, https://doi.org/10.3390/su12145747.

[26] D. Komnos, S. Tsiakmakis, J. Pavlovic, L. Ntziachristos, and G. Fontaras, "Analysing the real-world fuel and energy consumption of conventional and electric cars in Europe," *Energy Conversion and Management*, vol. 270, p. 116161, 2022, https://doi.org/10.1016/j.enconman.2022.116161.

[27] T. Wu, X. Han, M. M. Zheng, X. Ou, H. Sun, and X. Zhang, "Impact factors of the real-world fuel consumption rate of light duty vehicles in China," *Energy*, vol. 190, p. 116388, 2020, https://doi.org/10.1016/j.energy.2019.116388.

[28] A. M. Idris, A. F. Ramli, N. A. Burok, N. H. M. Nabil, Z. A. Muis, and H. W. Shin, "The Integration of Electric Vehicle with Power Generation Sector: A Scenario Analysis Based on Supply and Demand in Malaysia," *Materials Today: Proceedings*, vol. 19, pp. 1687-1692, 2019, https://doi.org/10.1016/j.matpr.2019.11.198.

[29] G. E. Kokieva, V. P. Druzyanova, and S. I. Grigoriev, "Research on the development of the agricultural sector of the Northern zone: repair and maintenance of machines," *IOP Conference Series: Earth and Environmental Science*, vol. 996, no. 1, p. 012030, 2022, https://doi.org/10.1088/1755-1315/996/1/012030.

[30] R. Makkar, B. E. Aalam, M. Jain, and A. wani, "A Review of Cost Analysis Study of Farm Tractor," *International Journal of Current Microbiology and Applied Sciences*, vol. 9, no. 3, pp. 2914-2921, 2020, https://doi.org/10.20546/ijcmas.2020.903.335.

[31] G. G. Han, J. H. Jeon, M. H. Kim, J. M. Lee, and S. M. Kim, "Comparison of Diesel Tractor Emissions in Korea," *Preprints*, 2021, https://doi.org/10.20944/preprints202112.0006.v1.

[32] Y. Ai *et al*., "Quantifying Air Pollutant Emission from Agricultural Machinery Using Surveys—A Case Study in Anhui, China," *Atmosphere*, vol. 12, no. 4, p. 440, 2021, https://doi.org/10.3390/atmos12040440.

[33] H. A. M. Khalid, H. Harun, A. M. Noor, and H. M. Hashim, "Green Human Resource Management, Perceived Organizational Support and Organizational Citizenship Behavior towards Environment in Malaysian Petroleum Refineries," *SHS Web of Conferences*, vol. 124, p. 11001, 2021, https://doi.org/10.1051/shsconf/202112411001.

[34] X. Guo *et al*., "Estimation and prediction of pollutant emissions from agricultural and construction diesel machinery in the Beijing-Tianjin-Hebei (BTH) region, China☆," *Environmental Pollution*, vol. 260, p. 113973, 2020, https://doi.org/10.1016/j.envpol.2020.113973.

[35] V. P. Aneja, W. H. Schlesinger, and J. W. Erisman, "Effects of Agriculture upon the Air Quality and Climate: Research, Policy, and Regulations," *Environmental Science & Technology*, vol. 43, no. 12, pp. 4234-4240, 2009, https://doi.org/10.1021/es8024403.

[36] B. S. Fakinle *et al*., "Spatial dispersion modeling of air emissions from a farm using a Gaussian model," *Environmental Quality Management*, vol. 31, no. 4, pp. 125-131, 2021, https://doi.org/10.1002/tqem.21752.

[37] P. C. Mishra, R. B. Ishaq, and F. Khoshnaw, "Mitigation strategy of carbon dioxide emissions through multiple muffler design exchange and gasoline-methanol blend replacement," *Journal of Cleaner Production*, vol. 286, p. 125460, 2021, https://doi.org/10.1016/j.jclepro.2020.125460.

[38] IARC Working Group on the Evaluation of Carcinogenic Risks to Humans, "Diesel and gasoline engine exhausts and some nitroarenes," *IARC monographs on the evaluation of carcinogenic risks to humans*, vol. 105, no. 9, 2014, https://www.ncbi.nlm.nih.gov/books/NBK531294/.

[39] S. Lakhani, N. Butani, and A. Kavad, "Severe Study of the Noise and Vibration Characteristics of an Agricultural Tractor," *International Journal of Current Microbiology and Applied Sciences*, vol. 9, no. 7, pp. 3187-3194, 2020, https://doi.org/10.20546/ijcmas.2020.907.372.

[40] A. Zanoletti, E. Carena, C. Ferrara, and E. Bontempi, "A Review of Lithium-Ion Battery Recycling: Technologies, Sustainability, and Open Issues," *Batteries*, vol. 10, no. 1, p. 38, 2024, https://doi.org/10.3390/batteries10010038.

[41] R. P. Sheth, N. S. Ranawat, A. Chakraborty, R. P. Mishra, and M. Khandelwal, "The Lithium-Ion Battery Recycling Process from a Circular Economy Perspective—A Review and Future Directions," *Energies*, vol. 16, no. 7, p. 3228, 2023, https://doi.org/10.3390/en16073228.

[42] L. Toro *et al*., "A Systematic Review of Battery Recycling Technologies: Advances, Challenges, and Future Prospects," *Energies*, vol. 16, no. 18, p. 6571, 2023, https://doi.org/10.3390/en16186571.

[43] H. Yang *et al*., "Life cycle assessment of secondary use and physical recycling of lithium-ion batteries retired from electric vehicles in China," *Waste Management*, vol. 178, pp. 168-175, 2024, https://doi.org/10.1016/j.wasman.2024.02.034.

[44] W. Wang and Y. Wu, "An overview of recycling and treatment of spent LiFePO4 batteries in China," *Resources, Conservation and Recycling*, vol. 127, pp. 233-243, 2017, https://doi.org/10.1016/j.resconrec.2017.08.019.

[45] P. Bhatt, H. Mehar, and M. Sahajwani, "Electrical Motors for Electric Vehicle – A Comparative Study," *SSRN Electronic Journal*, 2019, https://doi.org/10.2139/ssrn.3364887.

[46] M. G. Matache *et al*., "Small Power Electric Tractor Performance During Ploughing Works," *INMATEH Agricultural Engineering*, vol. 60, no. 1, pp. 123-129, 2020, https://doi.org/10.35633/inmateh-60-14.

[47] I. I. Hdaib, J. A. Yamin, "Analysis of Internal Combustion Engine Performance Using Design of Experiment," *Tehnički vjesnik*, vol. 29, no. 2, pp. 483-496, 2022, https://doi.org/10.17559/tv-20210312194600.

[48] K. Poornesh, K. P. Nivya and K. Sireesha, "A Comparative study on Electric Vehicle and Internal Combustion Engine Vehicles," *2020 International Conference on Smart Electronics and Communication (ICOSEC)*, pp. 1179-1183, 2020, https://doi.org/10.1109/ICOSEC49089.2020.9215386.

[49] H. Hong, G. B. Parvate-Patil, and B. Gordon, "Review and analysis of variable valve timing strategies—eight ways to approach," *Proceedings of the Institution of Mechanical Engineers, Part D: Journal of Automobile Engineering*, vol. 218, no. 10, pp. 1179-1200, 2004, https://doi.org/10.1177/095440700421801013.

[50] D. Troncon and L. Alberti, "Case of Study of the Electrification of a Tractor: Electric Motor Performance Requirements and Design," *Energies*, vol. 13, no. 9, p. 2197, 2020, https://doi.org/10.3390/en13092197.

[51] A. O. Polat, B. C. Erden, S. Kul, and F. Nasiroglu, "Light Electric Vehicle Performance with Digital Twin Technology: A Comparison of Motor Types," *Arabian Journal for Science and Engineering*, vol. 49, no. 5, pp. 7209-7222, 2024, https://doi.org/10.1007/s13369-023-08668-x.

[52] E. I. Deryabin and L. A. Zhuravleva, "Electric traction drive of an agricultural tractor," *IOP Conference Series: Earth and Environmental Science*, vol. 548, no. 3, p. 032037, 2020, https://doi.org/10.1088/1755-1315/548/3/032037.

[53] K. Lee and M. Lee, "Fault-Tolerant Stability Control for Independent Four-Wheel Drive Electric Vehicle Under Actuator Fault Conditions," *IEEE Access*, vol. 8, pp. 91368-91378, 2020, http://dx.doi.org/10.1109/ACCESS.2020.2994530.

[54] D. Mohanraj *et al*., "A Review of BLDC Motor: State of Art, Advanced Control Techniques, and Applications," *IEEE Access*, vol. 10, pp. 54833-54869, 2022, https://doi.org/10.1109/ACCESS.2022.3175011.

[55] A. Lajunen, P. Sainio, L. Laurila, J. Pippuri-Mäkeläinen, and K. Tammi, "Overview of Powertrain Electrification and Future Scenarios for Non-Road Mobile Machinery," *Energies*, vol. 11, no. 5, p. 1184, 2018, https://doi.org/10.3390/en11051184.

[56] P. Q. Khanh, V.-A. Truong, and H. P. H. Anh, "Extended Permanent Magnet Synchronous Motors Speed Range Based on the Active and Reactive Power Control of Inverters," *Energies*, vol. 14, no. 12, p. 3549, 2021, https://doi.org/10.3390/en14123549.

[57] Q. Chen, S. Kang, L. Zeng, Q. Xiao, C. Zhou, and M. Wu, "PMSM control for electric vehicle based on fuzzy PI," *International Journal of Electric and Hybrid Vehicles*, vol. 12, no. 1, p. 75, 2020, https://dx.doi.org/10.1504/ijehv.2020.104251.

[58] Y. Su, "Comparative Analysis of Lithium Iron Phosphate Battery and Ternary Lithium Battery," *Journal of Physics: Conference Series*, vol. 2152, no. 1, p. 012056, 2022, https://doi.org/10.1088/1742-6596/2152/1/012056.

[59] J. Shi, M. Tian, S. Han, T.-Y. Wu, and Y. Tang, "Electric Vehicle Battery Remaining Charging Time Estimation Considering Charging Accuracy and Charging Profile Prediction," *arXiv*, 2020, https://doi.org/10.48550/arxiv.2012.05352.

[60] E. Paffumi, M. D. Gennaro, and G. Martini, "In-vehicle battery capacity fade: A follow-up study on six European regions," *Energy Reports*, vol. 11, pp. 817-829, 2024, https://doi.org/10.1016/j.egyr.2023.12.026.

[61] A. Das, Y. Jain, M. R. B. Agrewale, Y. K. Bhateshvar and K. Vora, "Design of a Concept Electric Mini Tractor," *2019 IEEE Transportation Electrification Conference (ITEC-India)*, pp. 1-5, 2019, https://doi.org/10.1109/ITEC-India48457.2019.ITECINDIA2019-134.

[62] J. Liu *et al*., "Technical analysis of blending fusel to reduce carbon emission and pollution emission of diesel engine," *Fuel Processing Technology*, vol. 241, p. 107560, 2023, https://doi.org/10.1016/j.fuproc.2022.107560.

[63] B. A. Kolator, "Modeling of Tractor Fuel Consumption," *Energies*, vol. 14, no. 8, p. 2300, 2021, https://doi.org/10.3390/en14082300.

[64] Z. Sun, Z. Wen, X. Zhao, Y. Yang, and S. Li, "Real-World Driving Cycles Adaptability of Electric Vehicles," *World Electric Vehicle Journal*, vol. 11, no. 1, p. 19, 2020, https://doi.org/10.3390/wevj11010019.

[65] M. Z. Afzal *et al*., "A Novel Electric Vehicle Battery Management System Using an Artificial Neural Network-Based Adaptive Droop Control Theory," *International Journal of Energy Research*, vol. 2023. pp. 1-15, 2023, https://doi.org/10.1155/2023/2581729.

[66] I. Shishkin and S. Lushchin, "Controlling electrical circuit of electric motor on igbt transistors," *Electrical Engineering and Power Engineering*, pp. 30-35, 2023, https://doi.org/10.15588/1607-6761-2023-1-3.

[67] M. Gordić, D. Stamenković, V. Popović, S. Muždeka, A. Mićovi, "Electric vehicle conversion: optimisation of parameters in the design process," *Tehnicki vjesnik - Technical Gazette*, vol. 24, no. 4, pp. 1213-1219, 2017, https://doi.org/10.17559/tv-20160613131757.

[68] L. N. Patil *et al*., "Finite Element Analysis for Improved All-Terrain Vehicle Component Design," *Evergreen*, vol. 10, no. 3, pp. 1508-1521, 2023, https://doi.org/10.5109/7151699.

[69] F. Ballo, M. Gobbi, G. Mastinu, and R. Palazzetti, "Noise and Vibration of Permanent Magnet Synchronous Electric Motors: A Simplified Analytical Model," *IEEE Transactions on Transportation Electrification*, vol. 9, no. 2, pp. 2486-2496, 2023, https://doi.org/10.1109/tte.2022.3209917.

[70] J. Oh, M. Lee, E. Ko, K. M. Kim, and J. Kim, "Comprehensive understanding of the effects of imbalanced cell via battery module tests for further usage of cycled batteries," *Journal of Power Sources*, vol. 631, p. 236282, 2025, https://doi.org/10.1016/j.jpowsour.2025.236282.

[71] P. Q. Khanh and H. P. H. Anh, "Advanced PMSM speed control using fuzzy PI method for hybrid power control technique," *Ain Shams Engineering Journal*, vol. 14, no. 12, p. 102222, 2023, https://doi.org/10.1016/j.asej.2023.102222.

[72] K. Thangarajan and A. Soundarrajan, "Performance comparison of permanent magnet synchronous motor (PMSM) drive with delay compensated predictive controllers," *Microprocessors and Microsystems*, vol. 75, p. 103081, 2020, https://doi.org/10.1016/j.micpro.2020.103081.

[73] I. Hermawan, M. Ashari, and D. Riawan, "PV Farm Ancillary Function for Voltage Sag Mitigation Caused by Inrush Current of an Induction Motor," *International journal of intelligent engineering and systems*, vol. 15, no. 6, pp. 325-336, 2022, https://doi.org/10.22266/ijies2022.1231.31.

[74] M. Hashem, M. Abdel-Salam, M. Nayel, and M. Th. El-Mohandes, "Mitigation of voltage sag in a distribution system during start-up of water-pumping motors using superconducting magnetic energy storage: A case study," *Journal of Energy Storage*, vol. 55, p. 105441, 2022, https://doi.org/10.1016/j.est.2022.105441.

[75] M. Khamies, M. Abdel-Salam, A. Kassem, M. Nayel, M. El-Ghazaly, and M. Hashem, "Evaluating supercapacitor energy storage for voltage sag minimization in a real distribution feeder," *Journal of Energy Storage*, vol. 101, p. 113742, 2024, https://doi.org/10.1016/j.est.2024.113742.

[76] Y. Zhang, Z. Zhu, Z. Deng, and M. Wang, "Research on the impact of voltage sag characteristics in China on electric vehicle charging: BMW Brilliance Electric Vehicle as an example," *Electric Power Systems Research*, vol. 226, p. 109894, 2024, https://doi.org/10.1016/j.epsr.2023.109894.

[77] I. Miri, A. Fotouhi, and N. Ewin, "Electric vehicle energy consumption modelling and estimation—A case study," *International Journal of Energy Research*, vol. 45, no. 1, pp. 501-520, 2020, https://doi.org/10.1002/er.5700.

[78] Š. Lončarević, P. Ilinčić, G. Šagi, and Z. Lulić, "Problems and Directions in Creating a National Non-Road Mobile Machinery Emission Inventory: A Critical Review," *Sustainability*, vol. 14, no. 6, p. 3471, 2022, https://doi.org/10.3390/su14063471.

[79] R. Hagan *et al*., "Non-Road Mobile Machinery Emissions and Regulations: A Review," *Air*, vol. 1, no. 1, pp. 14-36, 2022, https://doi.org/10.3390/air1010002.

[80] Z. Shao and T. Dallmann, "European Stage V non-road emission standards," *International Council on Clean Transportation*, 2016, https://theicct.org/publication/european-stage-v-non-road-emission-standards/.

[81] M. Czechlowski, "Effect of Diesel Fuel Temperature on the Nitrogen Oxides Emission from a Compression-Ignition Engine," *Journal of Ecological Engineering*, vol. 21, no. 3, pp. 164-170, 2020, https://doi.org/10.12911/22998993/118283.

[82] M. Tkaczyk, Z. J. Sroka, K. Krakowian, and R. Wlostowski, "Experimental Study of the Effect of Fuel Catalytic Additive on Specific Fuel Consumption and Exhaust Emissions in Diesel Engine," *Energies*, vol. 14, no. 1, p. 54, 2020, https://doi.org/10.3390/en14010054.

[83] S. S. Karakulak and E. Yetkin, "Agricultural Tractor Cabin Safety Analysis and Test Correlation," *International Journal of Automotive Science and Technology*, vol. 4, no. 1, pp. 1-9, 2020, https://doi.org/10.30939/ijastech..641569.